

This is a PDF file of an article that is not yet the definitive version of record. This version will undergo additional copyediting, typesetting and review before it is published in its final form, but we are providing this version to give early visibility of the article. Please note that, during the production process, errors may be discovered which could affect the content, and all legal disclaimers that apply to the journal pertain. The final authenticated version is available online at: <https://doi.org/10.1016/j.molp.2023.06.004>

For the purpose of Open Access, the author has applied a CC BY public copyright licence to any Author Accepted Manuscript version arising from this submission.

This work was funded by European Research Council (POPMET project 834923).

QT-GWAS: a novel method for unveiling biosynthetic loci affecting qualitative metabolic traits

Marlies Brouckaert^{1,2,11,12}, Meng Peng^{1,2,12}, René Höfer^{1,2,3}, Ilias El Houari^{1,2}, Chiarina Darrah^{1,2,4}, Véronique Storme^{1,2,5}, Yvan Saeys^{6,7}, Ruben Vanholme^{1,2}, Geert Goeminne^{1,2,8}, Vitaliy I. Timokhin⁹, John Ralph⁹, Kris Morreel^{1,2,10} and Wout Boerjan^{1,2,*}

¹Ghent University, Department of Plant Biotechnology and Bioinformatics, Ghent, Belgium

² VIB Center for Plant Systems Biology, Ghent, Belgium

³ current address: BioNTech SE, Mainz, Rhineland-Palatinate, Germany

⁴ current address: Eunomia Research & Consulting, Bristol, United Kingdom.

⁵ current address: VIB Agro-incubator, Nevele, Belgium

⁶ Ghent University Department of Applied Mathematics, Computer Science and Statistics, Ghent, Belgium.

⁷ VIB Center for Inflammation Research, Ghent, Belgium.

⁸ VIB Metabolomics Core, Ghent, Belgium

⁹ Department of Biochemistry, and U.S. Department of Energy Great Lakes Bioenergy Research Center, Wisconsin Energy Institute, University of Wisconsin-Madison, Madison, WI, USA

¹⁰ current address: Research Institute for Chromatography, Kortrijk, Belgium

¹¹ current addresses are ^{6,7}

¹² These authors contributed equally to this article

* Correspondence: Wout Boerjan (wout.boerjan@psb.vib-ugent.be)

Running title: Qualitative & quantitative mGWAS in Arabidopsis

Short summary:

A novel genome-wide association method to uncover biosynthetic loci underlying qualitative metabolic traits (designated as QT-GWAS) was developed and performed alongside a conventional quantitative metabolite GWAS (mGWAS). At least 26 of the associations found were supported by previous research and 8 associations involving three metabolic enzyme-encoding genes (*CYP706A5*, *UGT76C3* and *SULT202B1*) were newly confirmed, illustrating the power of the novel QT-GWAS.

ABSTRACT

Although the plant kingdom provides an enormous diversity of metabolites with potentially beneficial applications for humankind, a large fraction of these metabolites and their biosynthetic pathways remains unknown. Resolving metabolite structures and their biosynthetic pathways is key to gaining biological understanding and to allow metabolic engineering. In order to retrieve novel biosynthetic genes involved in specialized metabolism, we developed a novel untargeted system-wide method in *Arabidopsis thaliana*, subjecting qualitative metabolic traits to a genome-wide association study (designated as Qualitative Trait GWAS or QT-GWAS), along with the more conventional metabolite GWAS (mGWAS) that considers the quantitative variation of metabolites. As proof of the validity of the QT-GWAS and mGWAS, 23 and 15 of the retrieved associations were supported by previous research. Furthermore, seven gene-metabolite associations retrieved by QT-GWAS were confirmed in this study through reverse genetics combined with metabolomics and/or *in vitro* enzyme assays. As such, we established that CYTOCHROME P450 706A5 (CYP706A5) is involved in the biosynthesis of chroman derivatives, UGT76C3 is able to hexosylate guanine *in vitro* and *in planta*, and SULFOTRANSFERASE 202B1 (SULT202B1) catalyzes the sulfation of neolignans *in vitro*.

INTRODUCTION

Plant metabolism entails a complex network of biochemical pathways, in which enzymes perform conversions that connect a wide variety of structurally diverse metabolites. The diversity and abundance of metabolites can be considered as a phenotypic output of the genome (Contrepolis et al., 2016). The plant metabolome can be classified into the primary and secondary/specialized metabolome. The former describes the collection of metabolites involved in processes essential for growth and development, whereas the latter comprises a specialized assortment of metabolites that allow the proper functioning and adaptation of an organism in a particular environment. Many metabolites in the specialized metabolome offer a use for humankind. They can lead to the development of medicines (Bishayee and Sethi, 2016; Desborough and Keeling, 2017), or commercially valuable products such as cosmetics, dyes, and oils (Loza-Tavera, 1999; Shin et al., 2013; Rose et al., 2018;

Góral and Wojciechowski, 2020). They can also contribute attractive properties to food, improve feed quality (Ricachenevsky et al., 2019), and present agricultural benefits such as enhanced biotic (Fürstenberg-Hägg et al., 2013; Arbona and Gomez-Cadenas, 2016; Chowański et al., 2016) and abiotic stress tolerance (Varela et al., 2016; Peng et al., 2017), enhanced yield (Steenackers et al., 2019), or improved interaction with beneficial organisms such as pollinators (Dudareva et al., 2013) or micro-organisms (Bouwmeester et al., 2019). Exploring the genetic mechanisms controlling the abundances of such metabolites is therefore crucial for both fundamental biological understanding and the engineering of plants to enhance metabolic traits.

Because of the vast amount of both metabolites and the genes underlying their biosynthesis, systems-wide tools are often employed to unravel biosynthetic pathways of specialized metabolites (Desmet et al., 2021a). By exploiting natural genomic variation, genome-wide association studies (GWAS) permit the search for associations of genomic markers, such as single-nucleotide polymorphisms (SNPs), with phenotypic traits of interest. In case the traits are metabolite abundances, this procedure is referred to as metabolite GWAS (mGWAS). mGWAS has become a valuable tool for uncovering new and uncharacterized genes/pathways using either targeted or untargeted metabolomics. For example, in *Arabidopsis thaliana* (Arabidopsis), mGWAS led to the discovery of genes involved in biosynthetic pathways of both primary (Strauch et al., 2015; Wu et al., 2016; Angelovici et al., 2017) and specialized metabolism (Chan et al., 2010; Routaboul et al., 2012; Li et al., 2014). An mGWAS study on Arabidopsis employed under different environmental conditions led to a list of 70 candidate genes putatively involved in the metabolism of several metabolic classes, of which five genes were experimentally validated by means of reverse genetics (Wu et al., 2018). mGWAS has been successfully used to discover genes controlling natural variation of metabolite abundances in crop plants such as rice (Chen et al., 2014; Dong et al., 2015; Matsuda et al., 2015; Chen et al., 2016; Brotman et al., 2021), maize (Wen et al., 2014; Wen et al., 2015; Chen et al., 2016; Baseggio et al., 2020), wheat (Chen et al., 2020; Shi et al., 2020) and tomato (Nunes-Nesi et al., 2019; Alseekh et al., 2020; Tohge et al., 2020).

In mGWAS, the number of loci that significantly contribute to the variation in metabolite abundance is often lower for specialized metabolites than for primary metabolites

(Fernie and Tohge, 2017). Because of the highly polygenic basis underlying primary metabolism, loci determining variation in primary metabolism are often of relatively small effect (<30% for a given locus) (Schauer et al., 2008; Wen et al., 2015; Wu et al., 2016; Knoch et al., 2017), whereas for specialized metabolism, loci with larger effect sizes (>30%) can often be identified (Chen et al., 2014; Wen et al., 2014; Luo, 2015), suggesting that the abundance of such specialized metabolites is predominantly affected by only a small number of major genes. Many specialized metabolites are decorated derivatives of common core structures (Morreel et al., 2014; Wang et al., 2019). Because many of the genes involved in this variety of decorations are conserved only among the most closely related species, specialized metabolism pathways are likely the result of neo-functionalizations following tandem gene duplications (Moghe and Last, 2015). This allows the creation of novel specialized metabolites of which the abundance is affected mostly by those specific duplicated genes. Furthermore, specialized metabolic pathways tend to be less subjected to natural selection compared with primary metabolic pathways. In primary metabolism, a major selective pressure is generally enforced by the large metabolic flux requirements inherent to the crucial role of primary metabolites. This high selective pressure ensures high precision of metabolic conversions and catalytic efficiency of enzymes in primary metabolism (Mukherjee et al., 2015). Genes underlying primary metabolism therefore tend to be highly conserved across the plant kingdom (Weng, 2014). In contrast, the selective pressure on specialized metabolism drives the variation in secondary metabolites rather than flux increases (Mukherjee et al., 2015). For example, when a particular specialized metabolite is no longer required for a specific subpopulation of a certain species to thrive (e.g., when the species enters a new niche), this metabolite could completely disappear in that subpopulation as a result of the accumulation of mutations in biosynthetic genes for that specialized metabolite. Such metabolites then represent distinct features in a natural population, only occurring in specific accessions (Sotelo-Silveira et al., 2015). The presence/absence of such a metabolite can be considered as a qualitative rather than a quantitative trait. The absence of a qualitative metabolic trait can be expected to show monogenic inheritance, considering that a knock-out mutation in one of the biosynthetic genes, will result in the loss of that metabolite. Such inheritance facilitates the discovery of the underlying genes (Kushalappa and Gunnaiah, 2013). In addition, because of their major effect, it is reasonable to hypothesize that, when subjecting

qualitative metabolic traits to genetic analysis, biosynthetic genes can readily be identified. For example, surveying leaf sinapate ester profiles from 96 *Arabidopsis* accessions demonstrated that the Pna-10 accession, which accumulates sinapoylglucose instead of sinapoylmalate, is a natural deletion mutant of *SNG1* encoding sinapoylglucose:malate sinapoyltransferase (Li et al., 2010). Similarly, a novel flavonol phenylacyltransferase gene (*FPT2*) has been identified based on a targeted study of saiginols present only in a subset of the analyzed accessions (Tohge et al., 2016). The absence of flavonol 3-*O*-gentiobioside 7-*O*-rhamnoside in 42 out of 81 analyzed *Arabidopsis* accessions led to the identification of an acyl-glucose-dependent glucosyltransferase (*BGLU6*) (Ishihara et al., 2016). This rather limited number of examples illustrates that analyses of qualitative metabolic traits (metabolic traits that are absent in part of the studied population) can pinpoint enzyme-encoding genes that underlie these metabolic conversions. Here, we performed an untargeted association analysis of 4,479 qualitative metabolic traits (Qualitative Trait GWAS or QT-GWAS) and 1,147 quantitative metabolic traits (mGWAS) obtained from liquid-chromatography–mass spectrometry (LC-MS) chromatograms with 250K SNPs of 183 *Arabidopsis* accessions. Both methods enriched for genes labelled with “metabolic process” related GOterms, but QT-GWAS did so more significantly. When focussing on associations involving characterised metabolites, we found 30 valid associations retrieved by the QT-GWAS of which 23 were supported by previous research and seven (involving the three genes *UGT76C3*, *CYP706A5* and *SULT202B1*) were newly confirmed in this study. Our results show that through an untargeted QT-GWAS, valid gene–metabolite associations can be retrieved at the level of enzyme-encoding genes involved in metabolic conversions, and can retrieve new associations not found by mGWAS. This is, to our knowledge, the first time an untargeted GWAS approach has been combined with qualitative metabolic traits.

RESULTS

LC–MS based metabolic profiles

An LC–MS analysis was performed on methanol extracts prepared from 14-day-old seedlings belonging to 183 accessions (Supplemental Table 1). A total of 5,082 metabolic features (peaks) was detected across all chromatograms (Supplemental Data Set 1), of which 603 were detected in all accessions. The other 4,479 features

that were below the detection limit (ion intensity of 500 in this study) in at least 1 of the 183 accessions were considered as qualitative traits. Features with an average abundance above 500 and that were present in at least 100 accessions (to reduce the false-positive rate resulting from too-small sample sizes and to ensure a continuous distribution of quantitative traits across the used population), were selected as quantitative traits (Wu et al., 2018). Based on the applied filtering, 1,147 of the 5,082 features were selected as quantitative traits, 702 of which could be identified as both qualitative and quantitative traits in this study (Figure 1).

Associations between qualitative metabolic traits and SNP data

SNP data were used from a previously published 250K SNP data set (Horton et al., 2012) for the 183 selected *Arabidopsis* accessions. SNPs that were monomorphic in all accessions were removed from the data set. Significant associations of qualitative features with SNPs were retrieved by a Fisher's exact test using a P -value $<10^{-6}$ threshold. Of the 4,479 qualitative features, 709 features (16%) were involved in 53,464 associations. After a filtering step to remove (i) redundant associations between a particular feature and SNPs that are located within a 20-kb window (10 kb up- and 10 kb downstream of the most significant SNP) based on the average linkage disequilibrium (LD) size in *Arabidopsis* (Kim et al., 2007), and (ii) redundant associations between a particular SNP and features representing the same metabolite [most metabolites are represented by multiple features in LC-MS (Mahieu et al., 2016)], 515 features (hereafter referred to as metabolites) remained that were involved in 2,931 associations (Figure 1A, Supplemental Data Set 2). MS/MS spectra were recorded for 140 of the 515 metabolites, of which 57 were tentatively characterized (Supplemental Table 2) using the DynLib spectral database (Desmet et al., 2021b). The metabolites were characterized as glucosinolates (13 metabolites), (neo)lignans/oligolignols (11, of which 5 were found to be sulfated); flavonoids (6), jasmonates (5), organic acids (4), aromatic polyketides (3), phenylpropanoids (3), benzenoids/coumarins (2), lipids (2), purines (2), an amino acid (1), and others (5).

From the 515 metabolites, 397 (77%) were associated with one locus and 118 (23%) with multiple loci (Figure 2). Here a locus is defined as the 10-kb upstream and 10-kb downstream region of the associated SNP based on the average size of LD in *Arabidopsis*. Considering loci with 10 or more associated metabolites (threshold based

on the observed elbow in Supplemental Figure 1) as pleiotropic loci, 23 such loci (L1-23) of the 2931 loci were found of which 1, 2, 1, 4, and 15 loci mapped on chromosomes 1 to 5, respectively (Figure 3, Supplemental Table 3). The pleiotropic locus L17 showed 83 associations, the highest number of associations of all loci in this data set, of which seven involved characterized glucosinolates, known to be affected by the *METHYLTHIOALKYLMALATE 1 (MAM1)*, *MAM2* and *MAM3* genes within this locus (Textor et al., 2004).

Associations between quantitative metabolic traits and SNP data

Next, we investigated the continuous variation of metabolic features in our data set. For the 1,147 quantitative features, the average abundance across the five replicates of each accession was calculated, and these averages were then subjected to a quantitative mGWAS following the EMMAX procedure (Kang et al., 2010). A genomic locus was considered as significantly associated with a particular feature, when at least 1 SNP in that locus showed a P -value $<10^{-6}$ (the most significant SNP is then defined as the lead SNP) and at least an additional 5 of 40 SNPs in a region upstream and downstream of the lead SNP showed a P -value $\leq 10^{-3}$. When such associations were retrieved, an associated locus was defined as the window of SNPs still in LD (showing a significant association) with the lead SNP. In this way, 288 quantitative traits (of which 71 were also defined as qualitative traits), estimated to correspond to 248 metabolites after feature grouping, were associated with 577 loci (Figure 1, Supplemental Data Set 3). Of the 248 metabolites, 31 could be characterized, all of which were also present in the QT-GWAS data set. The characterized metabolites contained glucosinolates (10), jasmonates (5), (neo)lignans/oligolignols (4), organic acids (3), flavonoids (2), phenylpropanoids (2), purines (2), aromatic polyketides (2), and an amino acid (1). Of the quantitative traits, 223 (90%) had only one significant association, whereas 25 (10%) showed multiple associations (Figure 2).

For the mGWAS, six pleiotropic loci could be identified (involved in associations with ten or more metabolites; Supplemental Figure 2, Supplemental Table 4). Two of the six pleiotropic loci were shared with the QT-GWAS (L5 and L17). The four other pleiotropic loci (L24-27) were all situated on chromosome 5, surrounding the pleiotropic *MAM* locus (L17). Both L5 and L17 showed associations with glucosinolates and are both known to contribute to natural variation in glucosinolates (Kliebenstein et al.,

2001; Kroymann et al., 2001). Possibly, the association of various glucosinolates to L24-27 could be explained by the existence of an extended LD block surrounding the *MAM* locus in L17 (Chan et al., 2010), resulting in SNPs, which are further away from the *MAM* locus, to still be associated with glucosinolates. A detailed overview of the loci and corresponding associated characterized metabolites can be found in Supplemental Table 4.

Gene Ontology term enrichment and overlap analysis

To investigate whether the loci associated with the metabolic traits were enriched in genes involved in metabolic processes, a GOterm enrichment was performed for both approaches, using the PANTHER webtool. For the qualitative approach, 103 GOterms in the 'biological process' category were significantly enriched (Bonferroni corrected *P*-value <0.05), not counting the unclassified category. Of these, twenty two GOterms (21%), related to various metabolic processes (Supplemental Table 5). For the quantitative approach, 25 GOterms were significantly enriched, of which five involved metabolic processes (20%). Of these 25 GOterms, all but one ('seed development' – GO:0048316) were also enriched in the QT-GWAS (Supplemental Table 6). Consequently, all GOterms involving metabolic processes that were enriched in the mGWAS were also enriched in the QT-GWAS. Notably, all of these metabolic GOterms were more significantly enriched in the QT-GWAS, although the fold-changes of the enrichments were of similar size (Supplemental Table 7).

Of the 702 traits that were selected as both qualitative and quantitative metabolites, 71 traits yielded associations for both QT-GWAS and mGWAS. QT-GWAS and mGWAS retrieved 2556 and 529 unique genes for these 71 traits. Of these genes, 167 were retrieved by both methods. The overlap coefficient (Szymkiewicz–Simpson coefficient; the ratio of the intersection of both gene sets and the size of the smallest gene set, here the mGWAS genes) is 0.32. This indicates that only 32% of the genes retrieved by mGWAS (the smallest set) overlapped with the genes retrieved by QT-GWAS, suggesting that the QT-GWAS is able to retrieve new associations not found by mGWAS.

Proof of concept

Knowing the structure of a metabolite facilitates the search for candidate enzyme-encoding genes involved in its biosynthesis (e.g., glycosylated metabolites associated with genes encoding glycosyltransferases) – in many cases not even requiring full metabolite annotation if key functional groups can be identified. Therefore, all associations in the filtered QT-GWAS data set involving the 57 characterized metabolites were investigated (758 associations out of 2,931 associations, Figure 1; Supplemental Data Set 4). In order to pinpoint enzyme-encoding genes involved in metabolic processes, the QT-GWAS data set was further filtered for genes labeled with GOslim categories (high level summaries of related GOterms) related to metabolic processes. In this way, 291 associations with 34 metabolites remained. Of this selection, at least 23 associations involving 21 of the 34 metabolites were supported by published research (Table 1, Supplemental Results), demonstrating that the QT-GWAS approach allows to pinpoint enzyme-encoding genes affecting the biosynthesis of the associated metabolites. Similarly, in the mGWAS data set, 67 associations out of the 577 involved the 31 characterized metabolites. After filtering for genes labeled with GOslims related to metabolic processes, 62 associations remained involving the 31 metabolites (Supplemental Data Set 5). Of these 62 associations, at least 15 associations involving 14 of the 31 characterized metabolites were supported by published research (Table 1, Supplemental Results). Twelve of the supported associations overlapped between QT-GWAS and mGWAS.

Retrieving new candidate genes involved in metabolic pathways

Guided by structural information of the associated metabolites, seven associations involving three genes were selected for validation through comparative metabolome profiling of knockout mutants and/or *in vitro* enzyme assays. Of these seven validated associations, five were also retrieved by the mGWAS.

CYP7065A, a gene involved in chroman biosynthesis

Chroman derivatives are heterocyclic compounds sharing a chroman (benzodihydropyran) backbone. Chromans constitute various important plant metabolites such as tocopherols, known for their vitamin E activity. In addition, the chroman skeletal structure occurs in specialized metabolites such as flavonoids (Jiang

et al., 2020). In the characterized qualitative data set, the second most significant association (P -value = 7.12×10^{-26}) in the QT-GWAS with characterized metabolites, was found between 6-hydroxy-2-methoxy-2-(pentane-2',4'-dione-5'-C-hexoside)-chroman (metabolite **48**) and SNP 4_7310453 located in the 3' UTR of AT4G12310 (Supplemental Data Set 4, Figure 4A and 4B). This gene encodes a cytochrome P450 monooxygenase (CYP706A5) and was also identified as part of a pleiotropic locus (locus L7, Figure 3, Supplemental Table 3). Two neighboring genes, AT4G12300 and AT4G12320, also encode CYP706A proteins (CYP706A4 and CYP706A6, respectively). Furthermore, the locus contains two copper amine oxidase genes (AT4G12280 and AT4G12290). However, these two genes do not show expression at the seedling stage according to external datasets and were therefore excluded as candidate genes to be involved in the metabolism of metabolite **48**. According to the ATTED-II database (Obayashi et al., 2022), CYP706A5 is strongly co-expressed with CYP706A6, suggesting they may be involved in the same metabolic pathway. Via QT-GWAS, also the abundances of an isomer of metabolite **48**, i.e. metabolite **49**, as well as of 6-hydroxy-2-methoxy-2-(2'-propanone-C-hexoside)-chroman (metabolite **37**, Figure 4A), were associated with SNPs located in locus L7 (SNP 4_7309739, P -value = 3.44×10^{-23} and SNP 4_7310453, P -value = 1.12×10^{-23} , respectively; Figure 4C and 4D). In addition, metabolites **48** and **49** were also associated with SNP 4_7310453 located in L7 via mGWAS (Table 1, Supplemental Data Set 5). No significant association was found for metabolite **37** via mGWAS. Q-Q plots for metabolites **48**, **49** and **37** show a tail reflecting the small P -values of significantly associated SNPs and the SNPs in LD, as can be expected (Supplemental Figure 9). Nevertheless, the plots suggest an inflation of the P -values for QT-GWAS which could be the result of population structure. In conclusion, CYP706A4, A5 and A6 were considered as candidate genes underlying the variance in abundance of metabolites **48**, **49** and **37**.

In order to confirm the effect of L7 on the abundances of the chroman derivatives **37**, **48** and **49**, one homozygous T-DNA insertion mutant was obtained for CYP706A4 (*cyp706a4*; Figure 4E) and one for CYP706A5 (*cyp706a5*; Figure 4E). No T-DNA insertion mutant was available for CYP706A6. The reduction in expression of CYP706A4 and CYP706A5 was confirmed by RT-qPCR in the corresponding mutant lines (Figure 4F), while the expression of the three other CYP706A genes was not altered (Supplemental Figure 3). Comparative metabolite profiling of seedling

metabolic extracts from each of the homozygous mutants revealed significant reductions for metabolites **37**, **48** and **39** in *cyp706a5*, but not in *cyp706a4* (Figure 4G, Supplemental Data Set 6-7). These results support the hypothesis that the *CYP706A5* is involved in the production of chromans **37**, **48** and **49**, as predicted by the QT-GWAS approach.

UGT76C3, a gene involved in guanine glycosylation

Guanine is one of the five essential nucleobases that make up part of the building blocks of nucleic acids and are ubiquitous in all known life forms. Nucleobases such as guanine can be taken up from the environment (Girke et al., 2014) or can be released from nucleotides or nucleic acids (Barbado et al., 2018). Little is known about guanine biosynthesis and metabolism, especially in plants. Based on MS/MS spectral data, two metabolites were characterized as guanine hexoside derivatives (metabolites **28** and **22**; Figure 5A). In the QT-GWAS data set, the variations in both guanine hexoside pools were significantly associated with SNP 5_1776009 located in L28 on chromosome 5 (Figure 5B and 5C). This locus contains seven enzyme-encoding genes: *DEOXYHYPUSINE SYNTHASE (DHS, AT5G05920)*, *GUANYLYL CYCLASE 1 (GC1, AT5G05930)*, and five *UDP-GLYCOSYLTRANSFERASE* genes (*UGT76C1-5*). *DHS* is involved in hypusine synthesis from peptidyl-lysine, whereas *GC1* is described to catalyze the formation of guanosine 3',5'-cyclic monophosphate (cGMP) from guanosine 5'-triphosphate (GTP) (Ludidi and Gehring, 2003; Duguay et al., 2007). *UGT76C1* (AT5G05870) and *UGT76C2* (AT5G05860) are described cytokinin UGTs (Šmehilová et al., 2016). *UGT76C4* (AT5G05880) and *UGT76C5* (AT5G05890) are known nicotinate UGTs (Wang et al., 2011; Li et al., 2015). The function of *UGT76C3* (AT5G05900) has not been reported yet. In addition, the most significantly associated SNP is located in the coding sequence of *UGT76C3*, implying *UGT76C3* is the most likely candidate glycosyltransferase involved in the biosynthesis of the guanine hexoside derivatives. Analogous to the chroman derivatives, Q-Q plots for metabolites **22** and **28** show a tail reflecting the small *P*-values of significantly associated SNPs and the SNPs in LD, and indicate some inflation of the *P*-values for QT-GWAS (Supplemental Figure 10). The associations of L28 with metabolites **28** and **22** were also retrieved in the mGWAS (Table 1).

To independently confirm the association between the *UGT76C3* candidate gene and metabolites **22** and **28**, two homozygous T-DNA insertion lines were obtained for *UGT76C3* (*ugt76c3-1* and *ugt76c3-2*, Figure 5E). The reduced *UGT76C3* expression in the *ugt76c3* mutant lines was confirmed by RT-qPCR (Figure 5F), whereas the expression of the other *UGT76C* genes was not altered (Supplemental Figure 4). Comparative metabolite profiling of *ugt76c3-1* and *ugt76c3-2* versus WT seedling samples showed that metabolite **28** was completely absent in both mutants and metabolite **22** was significantly decreased in both mutants (ANOVA; $P_{\text{FDR}} < 0.05$) (Figure 5G and 5H, Supplemental Data Set 8-9). Root tissues of both mutant lines and WT plants were subjected to metabolic profiling, given the relatively high expression of *UGT76C3* in roots (based on external datasets and RT-qPCR, Supplemental Figure 4). These results were in agreement with the seedling metabolic profiling (Supplemental Data Set 10-11). These results support that *UGT76C3* is causal for the natural variation in the abundance of the associated guanine hexoside derivatives in Arabidopsis seedlings and suggest that the glycosylation of guanine, the first step of the proposed metabolic pathway, is catalyzed by *UGT76C3* (Figure 5D).

To further investigate whether *UGT76C3* catalyzes the glycosylation of guanine as suggested (Figure 5D), *UGT76C3* was expressed in *E. coli* and purified as GST-tagged *UGT76C3* recombinant protein (GST-*UGT76C3*) for enzymatic assays. Guanine was incubated with GST-*UGT76C3* in the presence of UDP-glucose as a sugar donor. In contrast to the negative control, the GST-*UGT76C3* reaction product gave rise to one peak at m/z 312.1, which was consistent with the theoretical monoisotopic mass of the guanine glucoside $[M-H]^-$ ion ($C_{11}H_{14}N_5O_6^-$; 312.09441 Da) (Figure 5I). The MS/MS fragmentation spectrum further showed a neutral loss of 162 Da, corresponding to the loss of a hexose (minus H_2O) moiety, indicating that the glucose moiety and guanine are *N*-linked, not *C*-linked. These observations demonstrate that *UGT76C3* can catalyze the *N*-glycosylation of guanine *in vitro*.

SULT202B1, a gene involved in neolignan sulfation

Sulfation of flavonoids has been reported in various studies (Teles et al., 2018) and several underlying genes have been reported in Arabidopsis (Klein and Papenbrock, 2004; Hashiguchi et al., 2014). However, genes responsible for the sulfation of neolignans remain unknown. Three sulfated neolignans, sulfo-G(8-O-4)FA (G stands

for coniferyl alcohol and FA for ferulic acid, metabolite **21**) and its isomer (metabolite **29**), and sulfo-G(8-O-4)SA (SA stands for sinapic acid, metabolite **44**) were characterized in this study (Figure 6A). In the QT-GWAS data set, metabolites **21** (SNP 3_16490051; P -value = 7.37×10^{-8} , Figure 6B) and **44** (SNP 3_16487258; P -value = 4.92×10^{-7} , Figure 6C), were associated with locus L29 that contains four genes: a nitrate transporter (*NRT2.6*; AT3G45060), a sulfotransferase (*SULT202B1*; AT3G45070) and two nucleoside triphosphate hydrolases (AT3G45080 and AT3G45090). The sulfotransferase *SULT202B1* has been reported to operate on flavonoids (Gidda and Varin, 2006; Hashiguchi et al., 2013). The associations of metabolites **21** and **44** with L29 suggest that *SULT202B1* could potentially act upon neolignans as well. Alternatively, the association could be the result of competition between neolignans and flavonoids for conjugation. Q-Q plots for metabolites **21** and **44** show a less profound tail, compared to the chroman and guanin derivatives under investigation as a result of the less significant associations (Supplemental Figure 11). In the mGWAS, an association between locus L29 and metabolites **21** and **29** (Figure 6, B and D) could be retrieved, but not with metabolite **44**, even though it was selected as quantitative trait as well.

To test whether *SULT202B1* is active on G(8-O-4)FA or G(8-O-4)SA as predicted, recombinant GST-tagged *SULT202B1* was produced in *E. coli* and purified for *in vitro* enzyme assays with chemically synthesized G(8-O-4)FA and G(8-O-4)SA (Supplemental Methods). G(8-O-4)FA and G(8-O-4)SA were tested as potential substrates (see methods), whereas the flavonol galangin was used as a positive control. As previously reported, *SULT202B1* displayed activity towards galangin (Gidda and Varin, 2006). When incubated with G(8-O-4)FA, the *SULT202B1* reaction product gave rise to two peaks exhibiting an m/z value and fragmentation spectrum corresponding to sulfo-G(8-O-4)FA (Figure 6E). Similarly, two sulfo-G(8-O-4)SA peaks were observed when G(8-O-4)SA was incubated with *SULT202B1* (Figure 6F). These observations illustrate that *SULT202B1* can catalyze the sulfation of G(8-O-4)FA and G(8-O-4)SA *in vitro*.

We assessed the effect of population structure correction for qualitative metabolites whose associations were supported by previous research or validated in this study through ASRgwas (Table 1). As expected, for all tested traits, the associations retrieved by QT-GWAS were less significantly detected by ASRgwas. Notably, 19 out

of the 30 validated associations retrieved by QT-GWAS were no longer deemed significant by ASRgwas (p -values $> 10^{-6}$) even though they have been experimentally validated in this study or were supported by previous research. These results suggest population structure correction is in some cases too conservative and could overlook the identification of real associations, as also noted by (Klasen et al., 2016). We visualized the potential influence of population structure on the associations retrieved by QT-GWAS, through Uniform Manifold Approximation and Projection for Dimension Reduction (UMAP, (McInnes et al., 2020)) (Supplemental Figure 5, Supplemental Results, Supplemental Methods).

DISCUSSION

QT-GWAS and mGWAS both retrieve loci involved in the biosynthesis of specialized metabolites and are partially complementary

Several studies have illustrated that targeted genetic analyses of qualitative metabolic traits, only present in a subset of a population of accessions, can efficiently pinpoint biosynthetic genes (Li et al., 2010; Ishihara et al., 2016; Tohge et al., 2016). Such discoveries are highly important both for fundamental knowledge and to open up possibilities towards metabolic engineering. By performing an untargeted association analysis through Fisher's exact tests of 4,479 qualitative metabolic traits and 250K SNPs in *Arabidopsis*, we retrieved 2,931 significant associations with 515 metabolites (11% of all qualitative traits defined here). In comparison, mGWAS yielded 577 associations involving 248 (22% of 1147) quantitative metabolites. Considering that QT-GWAS and mGWAS picked up at least 23 and 15 literature-supported associations, respectively, both mGWAS and QT-GWAS methods are valid approaches to retrieve associations involved in the biosynthesis of specialized metabolites. The complementarity of both methods is illustrated by the observation that only twelve of the supported associations overlapped between both methods. Of the eight novel associations confirmed in this study, only five were retrieved by both methods.

The complementarity between both approaches could be explained by the fact that the QT-GWAS differentiates between genotypes in which the trait is absent and those

expressing the trait, whereas mGWAS narrows associations down to those genotypes affecting the trait quantitatively rather than qualitatively. Nevertheless, the complementarity could also in part be explained by the different selection criteria for qualitative and quantitative traits. However, for the traits that were selected both as quantitative and qualitative traits, the two methods yielded different results in agreement with the different statistical strategies of both methods (only 32% of the genes overlapped based on the Szymkiewicz–Simpson coefficient). For example, QT-GWAS was able to retrieve a correct association between 6-hydroxy-2-methoxy-2-(2'-propanone-C-hexoside)-chroman (metabolite **37**) and *CYP705A6* and between sulfo-G(8-O-4)SA (metabolite **44**) and *SULT202B1*, which were not retrieved by mGWAS at the current threshold, even though both metabolites were also selected as quantitative traits for the mGWAS. QT-GWAS was able to retrieve 11 associations that were supported by previous research that were not retrieved by mGWAS, despite the fact that the involved metabolites were used as input in both methods. Analogously, mGWAS yielded three literature-supported associations that were not found by QT-GWAS. The complementarity could (in part) be the result of the exclusion of rare alleles (minor allele frequency <5%) from mGWAS. Such alleles were not excluded from the QT-GWAS.

An enrichment for 'metabolic process'-related GOterms was observed for both the mGWAS and the QT-GWAS. The QT-GWAS showed a more significant enrichment for all 5 'metabolic process'-related GOterms that were enriched in the mGWAS, and also for 17 additional 'metabolic process'-related GOterms that were not enriched in the mGWAS. These results further support that the novel QT-GWAS is indeed able to retrieve genes involved in metabolism.

Novel enzyme–metabolite associations

In order to further demonstrate the validity of the QT-GWAS approach, candidate genes of unknown function were selected from genomic loci associated with characterized metabolites and subjected to reverse genetics. Comparative metabolic profiling of the T-DNA insertion mutant in candidate *CYP706A5* versus the WT showed that the abundance of the associated chroman derivatives **37**, **48** and **49** were significantly reduced in *cyp706a5*, indicating that *CYP706A5* is involved in the biosynthesis of these metabolites. Furthermore, these metabolites were not differential

in *cyp706a4*, indicating that the functions of CYP706A4 and CYP706A5 are not redundant. Metabolites **37**, **48** and **49** have previously been reported to be highly abundant in leaf vacuoles of Arabidopsis (Dima et al., 2015). Moreover, the putative structures of the associated metabolites **37**, **48** and **49** resemble polyketide synthase derailment products, because of their putative polyketide like nature (Yamaguchi et al., 1999; Jiang et al., 2006; Lim et al., 2016). Most polyketide synthases are promiscuous in the number of elongation steps, causing some polyketide intermediates to derail, resulting in heterocyclic truncation products (Lim et al., 2016). Although the involvement of CYP706A5 in the production of metabolites **37**, **48**, and **49** was demonstrated by reverse genetics, the identity of its *in vivo* substrate remains unclear.

Similarly, the metabolite profiling of T-DNA insertion lines in *UGT76C3*, located in L28, confirmed the involvement of the UGT in the production of metabolites **22** and **28**, as predicted by both the QT-GWAS and mGWAS. The biosynthesis of metabolites **22** and **28** could potentially start from the hexosylation of guanine by UGT76C3 (Figure 5D). This hypothesis is supported by the *in vitro* enzyme assay, which illustrates that UGT76C3 is indeed capable of catalyzing the glycosylation of guanine *in vitro*. This is, to our knowledge, the first time that guanine glycosylation has been reported in plants. Here, guanine (benzoyl) hexoside (metabolite **28**) and guanine (benzoyl)sulfo-hexoside (metabolite **22**) were detected, instead of guanine hexoside. A possible reason is that guanine hexoside is rapidly conjugated with benzoate and/or sulfate. This may also explain why guanine hexoside has not been reported yet in other organisms. The guanine (benzoyl) hexoside and guanine (benzoyl) sulfo-hexoside could possibly be storage molecules, as molecules are frequently hexosylated for storage in the vacuole (Dima et al., 2015; Le Roy et al., 2016; Desmet et al., 2021b). Because *UGT76C3* is highly expressed in roots, it could play a role in storage of excess guanine. Guanine has been shown to be taken up from the environment (Girke et al., 2014), but could also play a role as a nitrogen storage form in nitrogen-poor or -fluctuating environments (Mojzeš et al., 2020).

The QT-GWAS and mGWAS suggested that in addition to flavonoids, *SULT202B1* could also catalyze the sulfation of neolignans, based on the observed associations with metabolites **21**, **29** and **44**. This hypothesis was confirmed by *in vitro* enzyme assays. This is, to our knowledge, the first report of an enzyme capable of catalyzing the sulfation of neolignans *in vitro*. The sulfation of neolignans could serve to improve

their solubility in water, which could possibly alter their sequestration and/or transport to the vacuole or cell wall (Routaboul et al., 2012). Alternatively, sulfation of specialized metabolites, such as neolignans, could be the result of an adaptation to a specific environment. For example, a strong correlation was observed between the occurrence of sulfated flavonoids and plants growing near aquatic environments rich in mineral salts. Hence, the binding of sulfate to flavonoids and neolignans could be a mechanism for deactivation of excessive inorganic sulfate (Li et al., 2014).

QT-GWAS and mGWAS generate valuable databases

The QT-GWAS and mGWAS data sets retrieved a total of 26 literature-supported associations. Furthermore eight novel associations were confirmed here. These results illustrate that both methods lead to valuable gene–metabolite associations. In the QT-GWAS data set, 1,057 associations involved unknown metabolites and contained genes categorized under GOslims categories related to metabolic processes (Figure 1). In the list of QT-GWAS associations with characterized metabolites, at least 30 of the 291 associations (10%) involving metabolic genes were validated (23 through previous research and seven in this study). Extrapolating this percentage to the unknown associations, at least another 106 associations are promising leads. Analogously, in the mGWAS data set, 450 associations involved unknown metabolites and contained genes labeled with GOslims related to metabolic processes. In the mGWAS associations with characterized metabolites, 21 of the 62 associations (34%) involving metabolic genes were validated (15 through previous research and six in this study). Extrapolating this percentage to the unknown associations, at least 153 associations are predicted as promising leads. The 1,057 and 450 ‘metabolic process’-related loci involving unknown metabolites in QT-GWAS and mGWAS, respectively, can be mined further for additional candidate genes, which could be subjected to a combination of reverse genetics and metabolite profiling to investigate whether the abundance of the associated unknown metabolite is affected in the mutant. The identity of the potential substrate can be obtained through (partial) metabolite characterization, in case MS/MS spectral fragmentation data allows elucidation, isotope labeling (Simpson et al., 2021) or through purification and NMR analysis of the unknown metabolite.

METHODS

Plant growth and experimental setup

Seeds of 183 *A. thaliana* accessions (Supplemental Table 1) were sown on MS-agar plates (0.5X Murashige and Skoog medium, 0.5% (w/v) sucrose, 1.2% (w/v) plant tissue agar), and stratified at 4°C for five days. Based on a randomized block design, 14-day-old seedlings (five replicates per accession) were then transferred to 96-well plates (MultiScreen, Merck Millipore) with two seedlings per well in 1 mL liquid MS-medium (0.5X MS medium, 0.5% (w/v) sucrose). The 96-well plates were placed in a growth chamber for 12 days (21°C, 16 h light/8 h dark with 120 $\mu\text{Es}^{-1}\text{m}^{-2}$). For metabolite extraction, the growth medium was removed by vacuum filtration and samples were quenched with 1 mL dry-ice-cold methanol. After heating the samples to 70°C for 15 min, the methanol extract was collected in a receiver plate using a vacuum manifold. Subsequently, 500 μL of the collected extract was cleaned with a Sep-Pak C18 96-well plate (Waters), dried in a vacuum concentrator and suspended in 50 μL ultrapure water. The 250K SNP data was obtained from the Gregor Mendel Institute (available on github: https://github.com/Gregor-Mendel-Institute/atpolydb/tree/master/250k_snp_data).

All T-DNA insertion lines in this study were obtained from the SALK collection through the Nottingham Arabidopsis Stock Centre and homozygous mutants were identified by PCR amplification using T-DNA and gene specific primers (Supplemental Table 11). The Columbia-0 (Col-0) accession was used as WT.

Metabolite profiling and data processing

To obtain the metabolic profiles of all 183 *A. thaliana* accessions, each replicate (10 μL injected) was analyzed via negative ionization mode using a ultrahigh performance liquid chromatography (UHPLC) system hyphenated to electrospray ionization (ESI)-quadrupole-time of flight (QTOF)-MS (Acquity UPLC system coupled to a Synapt High Definition MS, Waters Corporation, Manchester, UK, Supplemental Methods). T-DNA insertion lines were analyzed on a Vion QTOF-MS (Waters Corporation, Manchester, UK, Supplemental Methods).

Peak grouping on the recorded LC–MS peaks was performed following Morreel et al. (2014) to estimate the number of detected metabolites. Statistical tests were performed

in R version 4.0.0 (R Core Team, 2020). Data were transformed as described previously (Desmet et al., 2021b). Significant differences in the feature abundances between the T-DNA mutant lines and the WT were obtained following a one-way analysis of variance (ANOVA; *lm()* function) followed by Tukey honestly significant difference [HSD; *TukeyHSD()*] post hoc tests ($\alpha=0.05$). The ANOVA model *P*-values were subjected to a false discovery rate [FDR, $P_{FDR}<0.05$; *p.adjust()*] correction.

MS-based structural elucidation

In addition to MS/MS spectra recorded via QTOF-MS, MSⁿ spectra were generated via reversed-phase UHPLC-ESI-Fourier transform ion cyclotron resonance (FTICR)-MS (Accela UHPLC system coupled to an LTQ FT Ultra, Thermo Scientific, Bremen, Germany) using the same separation conditions as mentioned for the QTOF-MS-based analyses. MS settings were as previously described (Desmet et al., 2021b). The MS/MS and MSⁿ spectra mutually aligned and interpreted using RDynLib (Desmet et al., 2021b). Spectral interpretation was further assisted using CSI:FingerID (Dührkop et al., 2015) and competitive fragmentation modeling (CFM)-ID (Allen et al., 2014), and by applying previously published MS fragmentation pathways (Morreel et al., 2006; Morreel et al., 2010a; Morreel et al., 2010b; Desmet et al., 2021b) (Supplemental Methods).

GWAS of qualitative traits (QT-GWAS)

LC-MS processed features were converted to binary traits and subjected to Fisher exact tests using R version 4.0.0 [R Core Team, 2020; see “Qualitative GWAS.R available on Github”]. Whenever a feature was absent in more than half of the replicates for a particular accession (3 or more out of 5), the feature was considered absent in that accession. Some 4,479 features remained for the QT-GWAS (after removing features either present or absent in all 183 accessions). Using the 250K SNP data set, cosegregation analysis between the presence/absence of a feature and the presence/absence of a SNP was performed with Fisher exact tests [*fisher.test()*; $-\log_{10}(P\text{-value}) > 6$] (see “Qualitative GWAS.R”). To accommodate for multiple hypotheses testing a *P*-value threshold of $P\text{-value} < 10^{-6}$ was selected to define associations as significant. All scripts are made available at Github (<https://github.com/mabro7766/QT>). Manhattan and Q-Q plots were generated with the “qqman” package in R (Turner, 2014).

GWAS of quantitative traits (mGWAS)

mGWAS was performed on metabolite abundances measured in the 183 selected *A. thaliana* accessions. *m/z* signals with an average abundance lower than the detection limit of 500 were put to missing. The analysis was limited to those metabolites where at least 100 accessions had a value above the detection limit. Only SNPs were considered with a minor allele fraction (MAF) of at least 0.05. The association study was performed analogous to Kang et al. (2010), see Supplemental Methods for detailed descriptions. To accommodate for multiple hypotheses testing correction a *P*-value threshold of *P*-value < 10⁻⁶ was selected to define associations as significant. All scripts are made available at Github (<https://github.com/mabro7766/mGWAS>).

Comparative GOterm analysis and overlap coefficient

Gene Ontology data was obtained from TAIR (<https://www.arabidopsis.org/>). A GOterm enrichment was performed using the PANTHER webtool (<http://pantherdb.org/>) for both QT-GWAS and mGWAS. The inputted genes included duplicates, [genes occurring in more than one association were included in the enrichment as many times as they showed associations (13,795 genes for the QT-GWAS and 3,535 genes for the mGWAS)]. Enrichment was assessed versus all Arabidopsis genes present in the database through Bonferroni-corrected Fisher's exact tests. The overlap coefficient (Szymkiewicz–Simpson) was calculated as ratio of the intersection and the size of the mGWAS gene set (equation 1).

$$(1) \text{ overlap}(A, B) = \frac{|A \cap B|}{\min(|A|, |B|)}$$

Gene expression analysis via RT-qPCR and external datasets

Shoot or root tissues of 2-week-old Arabidopsis seedlings were collected and immediately frozen in liquid nitrogen. Six plants were pooled per biological replicate and three replicates were harvested per line. All plant materials were disrupted in 2-mL Eppendorf tubes using a Retsch MM300 mill (20 Hz, 3-mm bead). Total RNA was extracted using ReliaPrep RNA Tissue Miniprep System (Promega). A total of 1 µg RNA was used as a template for cDNA synthesis using the qScript cDNA SuperMix (Quantabio). RT-qPCRs were performed using SYBR[®] Green Mix (Roche) in the Lightcycler[®] 480 System (Roche). Arabidopsis *UBIQUITIN CONJUGATION ENZYME 9* (*UBC9*, AT4G27960) and *UBC21* (AT5G25760) genes were used as reference

genes. Gene expression of AT4G12280, AT4G12290, AT4G12300, AT4G12310, AT4G12320, and AT5G05900 was checked via eFP browser (Winter et al., 2007).

Enzymatic assays

In vitro enzymatic assays of UGT76C3 were performed as described (Peng et al., 2017) enzymatic assays of SULT202B1 were conducted as described (Hashiguchi et al., 2013). Recombinant GST-tagged red fluorescent protein (RFP) was used as negative control. For recombinant protein expression and purification see Supplemental Methods.

LC–MS analyses of the reaction mixtures were performed on an Acquity UPLC system coupled to a Synapt-XS high resolution MS (Waters Corporation, Manchester, UK). Ten μ L reaction product was injected and analyzed as described for “Metabolite profiling and data processing” with the following altered parameter settings: desolvation temperature was set to 550°C, the desolvation gas flow was set to 800 L/h and transfer collision energy was set to 4 V.

SUPPLEMENTAL INFORMATION

Supplemental Information is available at *Molecular Plant Online*.

FUNDING

M.B. is indebted for funding to ERC-Advanced Grant 2019 POPMET and FWO-SB predoctoral fellowship (1S38920N), M.P. is indebted for funding to MSCA (CHORPATH – 897918), R.H. is indebted for funding to OMICS@VIB Marie Curie COFUND fellowship. I.E.H. is indebted for funding to FWO-SB predoctoral fellowship (1S04020N), EMBO research grant (STF-8658) and iBOF (Next-BIOREF, 01IB4220). We also thank the Bijzonder Onderzoeksfonds-Zware Apparatuur of Ghent University for the Fourier transform ion cyclotron resonance mass spectrometer (174PZA05) and the Hercules program of Ghent University for the Synapt QTOF High Definition MS (Grant AUGÉ/014). V.I.T. and J.R. were funded by the DOE Great Lakes Bioenergy Research Center (DOE BER Office of Science DE-SC0018409). W.B. is indebted for funding by Stanford University’s Global Climate and Energy Project ‘Towards New Degradable Lignin Types’ and by the ERC-Advanced Grant POPMET.

AUTHOR CONTRIBUTIONS

M.B., K.M. & W.B. designed the research; M.B., M.P., R.H., C.D. & I.E.H. performed experiments; M.B., K.M., V.S., & Y.S. developed scripts for data acquisition; V.I.T. and J.R. produced authentic synthetic compounds, M.B., M.P. & K.M. performed data analysis; M.B., M.P., K.M. & W.B. wrote the manuscript that all authors edited and approved.

ACKNOWLEDGMENTS

We would like to thank dr. engr. Joost Keurentjes for providing the *Arabidopsis* accessions and Marnik Vuylsteke (Gnomixx) for analyzing the data with the R packages ASRgwas and ASReml-R. We would like to thank Annick Bleys for critically reading the manuscript. No conflict of interest declared.

REFERENCES

- Allen, F., Pon, A., Wilson, M., Greiner, R., and Wishart, D.** (2014). CFM-ID: a web server for annotation, spectrum prediction and metabolite identification from tandem mass spectra. *Nucleic Acids Res.* **42**: W94-W99.
- Alseekh, S., Ofner, I., Liu, Z., Osorio, S., Vallarino, J., Last, R.L., Zamir, D., Tohge, T., and Fernie, A.R.** (2020). Quantitative trait loci analysis of seed-specialized metabolites reveals seed-specific flavonols and differential regulation of glycoalkaloid content in tomato. *Plant J.* **103**: 2007-2024.
- Angelovici, R., Batushansky, A., Deason, N., Gonzalez-Jorge, S., Gore, M.A., Fait, A., and DellaPenna, D.** (2017). Network-guided GWAS improves identification of genes affecting free amino acids. *Plant Physiol.* **173**: 872-886.
- Arbona, V., and Gomez-Cadenas, A.** (2016). Metabolomics of disease resistance in crops. *Curr. Issues Mol. Biol.* **19**: 13-30.
- Barbado, C., Córdoba-Cañero, D., Ariza, R.R., and Roldán-Arjona, T.** (2018). Nonenzymatic release of N7-methylguanine channels repair of abasic sites into an AP endonuclease-independent pathway in *Arabidopsis*. *Proc. Natl. Acad. Sci. USA* **115**: E916-E924.
- Baseggio, M., Murray, M., Magallanes - Lundback, M., Kaczmar, N., Chamness, J., Buckler, E.S., Smith, M.E., DellaPenna, D., Tracy, W.F., and Gore, M.A.** (2020). Natural variation for carotenoids in fresh kernels is controlled by uncommon variants in sweet corn. *Plant Genome* **13**: e20008.
- Bishayee, A., and Sethi, G.** (2016). Bioactive natural products in cancer prevention and therapy: progress and promise. *Semin. Cancer Biol.* **40-41**: 1-3.
- Bouwmeester, H., Schuurink, R.C., Bleeker, P.M., and Schiestl, F.** (2019). The role of volatiles in plant communication. *Plant J.* **100**: 892-907.
- Brotman, Y., Llorente - Wiegand, C., Oyong, G., Badoni, S., Misra, G., Anacleto, R., Parween, S., Pasion, E., Tiozon Jr, R.N., Anonuevo, J.J., et al.** (2021).

- The genetics underlying metabolic signatures in a brown rice diversity panel and their vital role in human nutrition. *Plant J.* **106**: 507-525.
- Chan, E.K.F., Rowe, H.C., and Kliebenstein, D.J.** (2010). Understanding the evolution of defense metabolites in *Arabidopsis thaliana* using genome-wide association mapping. *Genetics* **185**: 991-1007.
- Chen, J., Hu, X., Shi, T., Yin, H., Sun, D., Hao, Y., Xia, X., Luo, J., Fernie, A.R., He, Z., et al.** (2020). Metabolite-based genome-wide association study enables dissection of the flavonoid decoration pathway of wheat kernels. *Plant Biotechnol. J.* **18**: 1722-1735.
- Chen, W., Gao, Y., Xie, W., Gong, L., Lu, K., Wang, W., Li, Y., Liu, X., Zhang, H., Dong, H., et al.** (2014). Genome-wide association analyses provide genetic and biochemical insights into natural variation in rice metabolism. *Nat. Genet.* **46**: 714-721.
- Chen, W., Wang, W., Peng, M., Gong, L., Gao, Y., Wan, J., Wang, S., Shi, L., Zhou, B., Li, Z., et al.** (2016). Comparative and parallel genome-wide association studies for metabolic and agronomic traits in cereals. *Nat. Commun.* **7**: 12767.
- Chowański, S., Adamski, Z., Marciniak, P., Rosiński, G., Büyükgüzel, E., Büyükgüzel, K., Falabella, P., Scrano, L., Ventrella, E., Lelario, F., et al.** (2016). A review of bioinsecticidal activity of solanaceae alkaloids. *Toxins* **8**: 60.
- Contrepois, K., Liang, L., and Snyder, M.** (2016). Can metabolic profiles be used as a phenotypic readout of the genome to enhance precision medicine? *Clin. Chem.* **62**: 676-678.
- Desborough, M.J.R., and Keeling, D.M.** (2017). The aspirin story – from willow to wonder drug. *Br. J. Haematol.* **177**: 674-683.
- Desmet, S., Brouckaert, M., Boerjan, W., and Morreel, K.** (2021a). Seeing the forest for the trees: retrieving plant secondary biochemical pathways from metabolome networks. *Comp. Struct. Biotechnol. J.* **19**: 72-85.
- Desmet, S., Saeys, Y., Verstaen, K., Dauwe, R., Kim, H., Niculaes, C., Fukushima, A., Goeminne, G., Vanholme, R., Ralph, J., et al.** (2021b). Maize specialized metabolome networks reveal organ-preferential mixed glycosides. *Comp. Struct. Biotechnol. J.* **19**: 1127-1144.
- Dima, O., Morreel, K., Vanholme, B., Kim, H., Ralph, J., and Boerjan, W.** (2015). Small glycosylated lignin oligomers are stored in *Arabidopsis* leaf vacuoles. *Plant Cell* **27**: 695-710.
- Dong, X., Gao, Y., Chen, W., Wang, W., Gong, L., Liu, X., and Luo, J.** (2015). Spatiotemporal distribution of phenolamides and the genetics of natural variation of hydroxycinnamoyl spermidine in rice. *Mol. Plant* **8**: 111-121.
- Dudareva, N., Klempien, A., Muhlemann, J.K., and Kaplan, I.** (2013). Biosynthesis, function and metabolic engineering of plant volatile organic compounds. *New Phytol.* **198**: 16-32.
- Duguay, J., Jamal, S., Liu, Z., Wang, T.-W., and Thompson, J.E.** (2007). Leaf-specific suppression of deoxyhypusine synthase in *Arabidopsis thaliana* enhances growth without negative pleiotropic effects. *J. Plant Physiol.* **164**: 408-420.
- Dührkop, K., Shen, H.B., Meusel, M., Rousu, J., and Böcker, S.** (2015). Searching molecular structure databases with tandem mass spectra using CSI:FingerID. *Proc. Natl. Acad. Sci. USA* **112**: 12580-12585.
- Fernie, A.R., and Tohge, T.** (2017). The genetics of plant metabolism. *Annu. Rev. Genet.* **51**: 287-310.

- Fürstenberg-Hägg, J., Zagrobelny, M., and Bak, S.** (2013). Plant defense against insect herbivores. *Int. J. Mol. Sci.* **14**: 10242-10297.
- Gidda, S.K., and Varin, L.** (2006). Biochemical and molecular characterization of flavonoid 7-sulfotransferase from *Arabidopsis thaliana*. *Plant Physiol. Biochem.* **44**: 628-636.
- Girke, C., Daumann, M., Niopek-Witz, S., and Möhlmann, T.** (2014). Nucleobase and nucleoside transport and integration into plant metabolism. *Front. Plant Sci.* **5**: 443.
- Góral, I., and Wojciechowski, K.** (2020). Surface activity and foaming properties of saponin-rich plants extracts. *Adv. Colloid Interface Sci.* **279**: 102145.
- Hashiguchi, T., Sakakibara, Y., Hara, Y., Shimohira, T., Kurogi, K., Akashi, R., Liu, M.-C., and Suiko, M.** (2013). Identification and characterization of a novel kaempferol sulfotransferase from *Arabidopsis thaliana*. *Biochem. Biophys. Res. Commun.* **434**: 829-835.
- Hashiguchi, T., Sakakibara, Y., Shimohira, T., Kurogi, K., Yamasaki, M., Nishiyama, K., Akashi, R., Liu, M.-C., and Suiko, M.** (2014). Identification of a novel flavonoid glycoside sulfotransferase in *Arabidopsis thaliana*. *J. Biochem.* **155**: 91-97.
- Horton, M.W., Hancock, A.M., Huang, Y.S., Toomajian, C., Atwell, S., Auton, A., Mulyati, N.W., Platt, A., Sperone, F.G., Vilhjálmsson, B.J., et al.** (2012). Genome-wide patterns of genetic variation in worldwide *Arabidopsis thaliana* accessions from the RegMap panel. *Nat. Genet.* **44**: 212-216.
- Ishihara, H., Tohge, T., Viehöver, P., Fernie, A.R., Weisshaar, B., and Stracke, R.** (2016). Natural variation in flavonol accumulation in *Arabidopsis* is determined by the flavonol glucosyltransferase BGLU6. *J. Exp. Bot.* **67**: 1505-1517.
- Jiang, C., Schommer, C.K., Kim, S.Y., and Suh, D.Y.** (2006). Cloning and characterization of chalcone synthase from the moss, *Physcomitrella patens*. *Phytochemistry* **67**: 2531-2540.
- Jiang, S., Su, S., Chen, M., Peng, F., Zhou, Q., Liu, T., Liu, L., and Xue, W.** (2020). Antibacterial activities of novel dithiocarbamate-containing 4*H*-chromen-4-one derivatives. *J. Agric. Food Chem.* **68**: 5641-5647.
- Kang, H.M., Sul, J.H., Service, S.K., Zaitlen, N.A., Kong, S.-y., Freimer, N.B., Sabatti, C., and Eskin, E.** (2010). Variance component model to account for sample structure in genome-wide association studies. *Nat. Genet.* **42**: 348-354.
- Kim, S., Plagnol, V., Hu, T.T., Toomajian, C., Clark, R.M., Ossowski, S., Ecker, J.R., Weigel, D., and Nordborg, M.** (2007). Recombination and linkage disequilibrium in *Arabidopsis thaliana*. *Nat. Genet.* **39**: 1151-1155.
- Klasen, J.R., Barbez, E., Meier, L., Meinshausen, N., Bühlmann, P., Koornneef, M., Busch, W., and Schneeberger, K.** (2016). A multi-marker association method for genome-wide association studies without the need for population structure correction. *Nature communications* **7**: 13299.
- Klein, M., and Papenbrock, J.** (2004). The multi-protein family of *Arabidopsis* sulphotransferases and their relatives in other plant species. *J. Exp. Bot.* **55**: 1809-1820.
- Kliebenstein, D.J., Kroymann, J., Brown, P., Figuth, A., Pedersen, D., Gershenzon, J., and Mitchell-Olds, T.** (2001). Genetic control of natural variation in *Arabidopsis* glucosinolate accumulation. *Plant Physiol.* **126**: 811-825.
- Knoch, D., Riewe, D., Meyer, R.C., Boudichevskaia, A., Schmidt, R., and Altmann, T.** (2017). Genetic dissection of metabolite variation in *Arabidopsis* seeds:

- evidence for mQTL hotspots and a master regulatory locus of seed metabolism. *J. Exp. Bot.* **68**: 1655-1667.
- Kroymann, J., Textor, S., Tokuhisa, J.G., Falk, K.L., Bartram, S., Gershenzon, J., and Mitchell-Olds, T.** (2001). A gene controlling variation in Arabidopsis glucosinolate composition is part of the methionine chain elongation pathway. *Plant Physiol.* **127**: 1077-1088.
- Kushalappa, A.C., and Gunnaiah, R.** (2013). Metabolo-proteomics to discover plant biotic stress resistance genes. *Trends Plant Sci.* **18**: 522-531.
- Le Roy, J., Huss, B., Creach, A., Hawkins, S., and Neutelings, G.** (2016). Glycosylation is a major regulator of phenylpropanoid availability and biological activity in plants. *Front. Plant Sci.* **7**: 735.
- Li, W., Zhang, F., Chang, Y., Zhao, T., Schranz, M.E., and Wang, G.** (2015). Nicotinate O-glucosylation is an evolutionarily metabolic trait important for seed germination under stress conditions in *Arabidopsis thaliana*. *Plant Cell* **27**: 1907-1924.
- Li, X., Bergelson, J., and Chapple, C.** (2010). The *ARABIDOPSIS* accession Pna-10 is a naturally occurring *sng1* deletion mutant. *Mol. Plant* **3**: 91-100.
- Li, X., Svedin, E., Mo, H., Atwell, S., Dilkes, B.P., and Chapple, C.** (2014). Exploiting natural variation of secondary metabolism identifies a gene controlling the glycosylation diversity of dihydroxybenzoic acids in *Arabidopsis thaliana*. *Genetics* **198**: 1267-1276.
- Lim, Y.P., Go, M.K., and Yew, W.S.** (2016). Exploiting the biosynthetic potential of type III polyketide synthases. *Molecules* **21**: 806.
- Loza-Tavera, H.** (1999). Monoterpenes in essential oils. Biosynthesis and properties. *Adv. Exp. Med. Biol.* **464**: 49-62.
- Ludidi, N., and Gehring, C.** (2003). Identification of a novel protein with guanylyl cyclase activity in *Arabidopsis thaliana*. *J. Biol. Chem.* **278**: 6490-6494.
- Luo, J.** (2015). Metabolite-based genome-wide association studies in plants. *Curr. Opin. Plant Biol.* **24**: 31-38.
- Mahieu, N.G., Spalding, J.L., Gelman, S.J., and Patti, G.J.** (2016). Defining and detecting complex peak relationships in mass spectral data: the Mz.unity algorithm. *Anal. Chem.* **88**: 9037-9046.
- Matsuda, F., Nakabayashi, R., Yang, Z., Okazaki, Y., Yonemaru, J.-i., Ebana, K., Yano, M., and Saito, K.** (2015). Metabolome-genome-wide association study dissects genetic architecture for generating natural variation in rice secondary metabolism. *Plant J.* **81**: 13-23.
- McInnes, L., Healy, J., and Melville, J.** (2020). Umap: Uniform manifold approximation and projection for dimension reduction. arXiv:1802.03426.
- Moghe, G.D., and Last, R.L.** (2015). Something old, something new: conserved enzymes and the evolution of novelty in plant specialized metabolism. *Plant Physiol.* **169**: 1512-1523.
- Mojzeš, P., Gao, L., Ismagulova, T., Pilátová, J., Moudříková, S., Gorelova, O., Solovchenko, A., Nedbal, L., and Salih, A.** (2020). Guanine, a high-capacity and rapid-turnover nitrogen reserve in microalgal cells. *Proc. Natl. Acad. Sci. USA* **117**: 32722-32730.
- Morreel, K., Dima, O., Kim, H., Lu, F., Niculaes, C., Vanholme, R., Dauwe, R., Goeminne, G., Inzé, D., Messens, E., et al.** (2010a). Mass spectrometry-based sequencing of lignin oligomers. *Plant Physiol.* **153**: 1464-1478.
- Morreel, K., Goeminne, G., Storme, V., Sterck, L., Ralph, J., Coppieters, W., Breyne, P., Steenackers, M., Georges, M., Messens, E., et al.** (2006).

- Genetical metabolomics of flavonoid biosynthesis in *Populus*: a case study. *Plant J.* **47**: 224-237.
- Morreel, K., Kim, H., Lu, F., Dima, O., Akiyama, T., Vanholme, R., Niculaes, C., Goeminne, G., Inzé, D., Messens, E., et al.** (2010b). Mass spectrometry-based fragmentation as an identification tool in lignomics. *Anal. Chem.* **82**: 8095-8105.
- Morreel, K., Saeys, Y., Dima, O., Lu, F., Van de Peer, Y., Vanholme, R., Ralph, J., Vanholme, B., and Boerjan, W.** (2014). Systematic structural characterization of metabolites in *Arabidopsis* via candidate substrate-product pair networks. *Plant Cell* **26**: 929-945.
- Mukherjee, D., Mukherjee, A., and Ghosh, T.C.** (2015). Evolutionary rate heterogeneity of primary and secondary metabolic pathway genes in *Arabidopsis thaliana*. *Genome Biol. Evol.* **8**: 17-28.
- Nunes-Nesi, A., Alseikh, S., de Oliveira Silva, F.M., Omranian, N., Lichtenstein, G., Mirnezhad, M., González, R.R.R., Sabio y Garcia, J., Conte, M., Leiss, K.A., et al.** (2019). Identification and characterization of metabolite quantitative trait loci in tomato leaves and comparison with those reported for fruits and seeds. *Metabolomics* **15**: 46.
- Obayashi, T., Hibara, H., Kagaya, Y., Aoki, Y., and Kinoshita, K.** (2022). ATTED-II v11: a plant gene coexpression database using a sample balancing technique by subagging of principal components. *Plant Cell Physiol.* **63**: 869-881.
- Peng, M., Shahzad, R., Gul, A., Subthain, H., Shen, S., Lei, L., Zheng, Z., Zhou, J., Lu, D., Wang, S., et al.** (2017). Differentially evolved glucosyltransferases determine natural variation of rice flavone accumulation and UV-tolerance. *Nat. Commun.* **8**: 1975.
- R Core Team** (2020). R: a language and environment for statistical computing. Foundation for Statistical Computing, Vienna, Austria (<http://www.R-project.org/>).
- Ricachenevsky, F.K., Vasconcelos, M.W., Shou, H., Johnson, A.A.T., and Sperotto, R.A.** (2019). Editorial: Improving the nutritional content and quality of crops: promises, achievements, and future challenges. *Front. Plant Sci.* **10**: 738.
- Rose, P.M., Cantrill, V., Benohoud, M., Tidder, A., Rayner, C.M., and Blackburn, R.S.** (2018). Application of anthocyanins from blackcurrant (*Ribes nigrum* L.) fruit waste as renewable hair dyes. *J. Agric. Food Chem.* **66**: 6790-6798.
- Routaboul, J.-M., Dubos, C., Beck, G., Marquis, C., Bidzinski, P., Loudet, O., and Lepiniec, L.** (2012). Metabolite profiling and quantitative genetics of natural variation for flavonoids in *Arabidopsis*. *J. Exp. Bot.* **63**: 3749-3764.
- Schauer, N., Semel, Y., Balbo, I., Steinfath, M., Repsilber, D., Selbig, J., Pleban, T., Zamir, D., and Fernie, A.R.** (2008). Mode of inheritance of primary metabolic traits in tomato. *Plant Cell* **20**: 509-523.
- Shi, T., Zhu, A., Jia, J., Hu, X., Chen, J., Liu, W., Ren, X., Sun, D., Fernie, A.R., Cui, F., et al.** (2020). Metabolomics analysis and metabolite - agronomic trait associations using kernels of wheat (*Triticum aestivum*) recombinant inbred lines. *Plant J.* **103**: 279-292.
- Shin, S.W., Jung, E., Kim, S., Kim, J.-H., Kim, E.-G., Lee, J., and Park, D.** (2013). Antagonizing effects and mechanisms of afzelin against UVB-induced cell damage. *PLoS ONE* **8**: e61971.
- Simpson, J.P., Wunderlich, C., Li, X., Svedin, E., Dilkes, B., and Chapple, C.** (2021). Metabolic source isotopic pair labeling and genome-wide association

- are complementary tools for the identification of metabolite–gene associations in plants. *The Plant Cell* **33**: 492-510.
- Šmehilová, M., Dobrušková, J., Novák, O., Takáč, T., and Galuszka, P.** (2016). Cytokinin-specific glycosyltransferases possess different roles in cytokinin homeostasis maintenance. *Front. Plant Sci.* **7**: 1264.
- Sotelo-Silveira, M., Chauvin, A.-L., Marsch-Martinez, N., Winkler, R., and de Folter, S.** (2015). Metabolic fingerprinting of *Arabidopsis thaliana* accessions. *Front. Plant Sci.* **6**: 365.
- Steenackers, W., El Houari, I., Baekelandt, A., Witvrouw, K., Dhondt, S., Leroux, O., Gonzalez, N., Corneillie, S., Cesarino, I., Inzé, D., et al.** (2019). *cis*-Cinnamic acid is a natural plant growth-promoting compound. *J. Exp. Bot.* **70**: 6293-6304.
- Strauch, R.C., Svedin, E., Dilkes, B., Chapple, C., and Li, X.** (2015). Discovery of a novel amino acid racemase through exploration of natural variation in *Arabidopsis thaliana*. *Proc. Natl. Acad. Sci. USA* **112**: 11726-11731.
- Teles, Y.C.F., Souza, M.S.R., and de Souza, M.D.F.V.** (2018). Sulphated flavonoids: biosynthesis, structures, and biological activities. *Molecules* **23**: 480.
- Textor, S., Bartram, S., Kroymann, J., Falk, K.L., Hick, A., Pickett, J.A., and Gershenzon, J.** (2004). Biosynthesis of methionine-derived glucosinolates in *Arabidopsis thaliana*: recombinant expression and characterization of methylthioalkylmalate synthase, the condensing enzyme of the chain-elongation cycle. *Planta* **218**: 1026-1035.
- Tohge, T., Scossa, F., Wendenburg, R., Frasse, P., Balbo, I., Watanabe, M., Alseekh, S., Jadhav, S.S., Delfin, J.C., Lohse, M., et al.** (2020). Exploiting natural variation in tomato to define pathway structure and metabolic regulation of fruit polyphenolics in the lycopersicum complex. *Mol. Plant* **13**: 1027-1046.
- Tohge, T., Wendenburg, R., Ishihara, H., Nakabayashi, R., Watanabe, M., Sulpice, R., Hoefgen, R., Takayama, H., Saito, K., Stitt, M., et al.** (2016). Characterization of a recently evolved flavonol-phenylacyltransferase gene provides signatures of natural light selection in Brassicaceae. *Nat. Commun.* **7**: 12399.
- Turner, S.D.** (2014). qqman: an R package for visualizing GWAS results using QQ and manhattan plots. *Biorxiv*:10.1101/005165.
- Varela, M.C., Arslan, I., Reginato, M.A., Cenzano, A.M., and Luna, M.V.** (2016). Phenolic compounds as indicators of drought resistance in shrubs from Patagonian shrublands (Argentina). *Plant Physiol. Biochem.* **104**: 81-91.
- Wang, J., Ma, X.-M., Kojima, M., Sakakibara, H., and Hou, B.-K.** (2011). *N*-glucosyltransferase UGT76C2 is involved in cytokinin homeostasis and cytokinin response in *Arabidopsis thaliana*. *Plant Cell Physiol.* **52**: 2200-2213.
- Wang, S., Alseekh, S., Fernie, A.R., and Luo, J.** (2019). The structure and function of major plant metabolite modifications. *Mol. Plant* **12**: 899-919.
- Wen, W., Li, D., Li, X., Gao, Y., Li, W., Li, H., Liu, J., Liu, H., Chen, W., Luo, J., et al.** (2014). Metabolome-based genome-wide association study of maize kernel leads to novel biochemical insights. *Nat. Commun.* **5**: 3438.
- Wen, W., Li, K., Alseekh, S., Omerian, N., Zhao, L., Zhou, Y., Xiao, Y., Jin, M., Yang, N., Liu, H., et al.** (2015). Genetic determinants of the network of primary metabolism and their relationships to plant performance in a maize recombinant inbred line population. *Plant Cell* **27**: 1839-1856.
- Weng, J.-K.** (2014). The evolutionary paths towards complexity: a metabolic perspective. *New Phytol.* **201**: 1141-1149.

- Winter, D., Vinegar, B., Nahal, H., Ammar, R., Wilson, G.V., and Provart, N.J.** (2007). An “electronic Fluorescent Pictograph” browser for exploring and analyzing large-scale biological data sets. *PLoS ONE* **2**: e718.
- Wu, S., Alseekh, S., Cuadros-Inostroza, Á., Fusari, C.M., Mutwil, M., Kooke, R., Keurentjes, J.B., Fernie, A.R., Willmitzer, L., and Brotman, Y.** (2016). Combined use of genome-wide association data and correlation networks unravels key regulators of primary metabolism in *Arabidopsis thaliana*. *PLoS Genet.* **12**: e1006363.
- Wu, S., Tohge, T., Cuadros-Inostroza, Á., Tong, H., Tenenboim, H., Kooke, R., Méret, M., Keurentjes, J.B., Nikoloski, Z., Fernie, A.R., et al.** (2018). Mapping the *Arabidopsis* metabolic landscape by untargeted metabolomics at different environmental conditions. *Mol. Plant* **11**: 118-134.
- Yamaguchi, T., Kurosaki, F., Suh, D.Y., Sankawa, U., Nishioka, M., Akiyama, T., Shibuya, M., and Ebizuka, Y.** (1999). Cross-reaction of chalcone synthase and stilbene synthase overexpressed in *Escherichia coli*. *FEBS Lett.* **460**: 457-461.

Figures

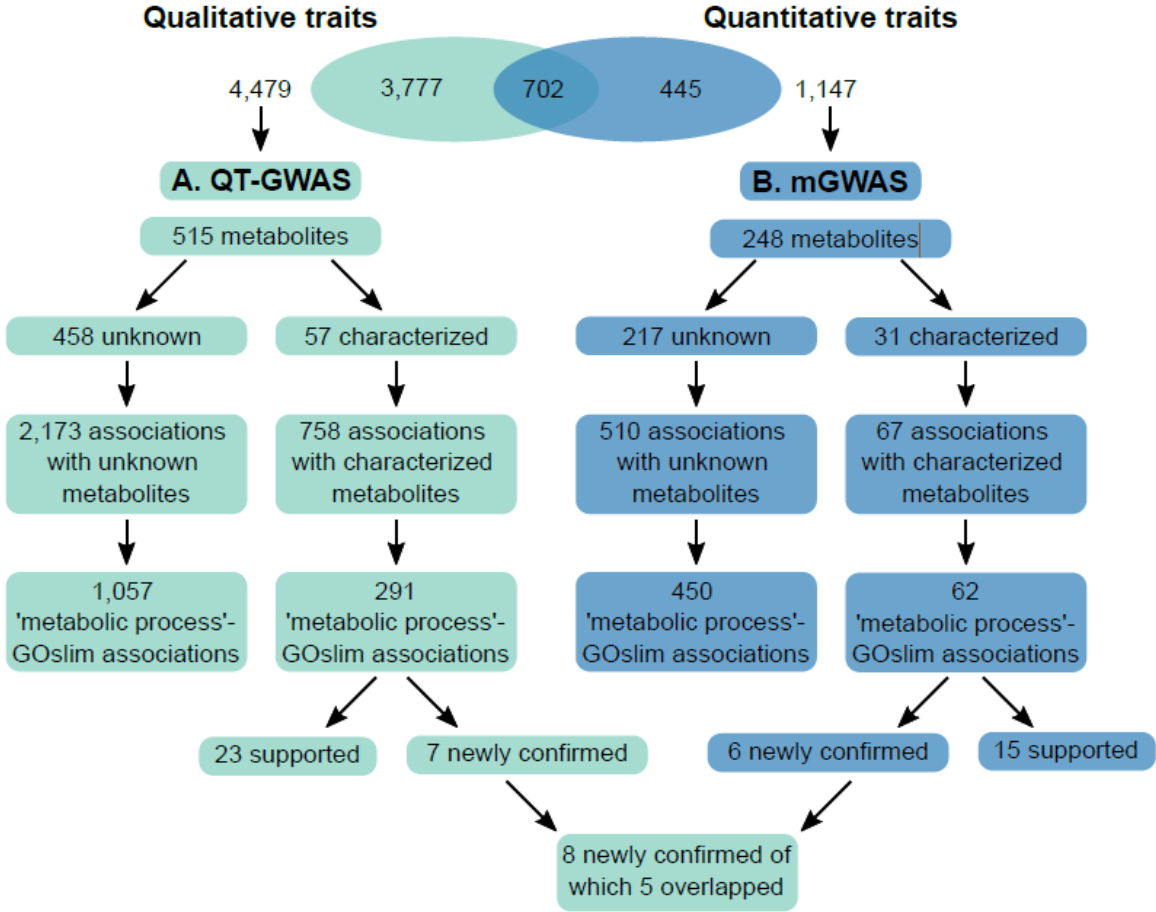


Figure 1: Schematic overview of the qualitative and quantitative traits and their recorded associations. A, 4,479 qualitative metabolic traits were used as input for the QT-GWAS. Associations were retrieved for 709 qualitative traits, estimated to correspond to 515 metabolites, of which 57 were characterized and 458 remained unknown. 2,173 associations were retrieved for the unknown metabolites, of which 1,057 involved loci encoding enzymes labeled with ‘metabolic process’-related GOslim categories. The 57 characterized metabolites were involved in 758 associations. In this dataset, 291 loci contained genes labeled with ‘metabolic process’-related GOslim categories. At least 23 of these associations were confirmed or supported by previous research and seven (involving three loci) were newly confirmed in this study. **B**, 1,147 quantitative traits were used as input for the mGWAS. Associations were retrieved for 288 of estimated to correspond to 248 metabolites. Of these metabolites, 31 were characterized and 217 remained unknown. The unknowns were involved in 510

associations of which 450 encompassed loci containing genes labeled with 'metabolic process'-related GOslim categories. The 31 characterized metabolites were involved in 67 associations. In this dataset, 62 loci contained genes labeled with 'metabolic process'-related GOslim categories, of which at least 15 were confirmed or supported by previous research and six (involving 3 loci) were newly confirmed in this study. In total, eight new associations were confirmed in this study of which five overlapped between the two methods.

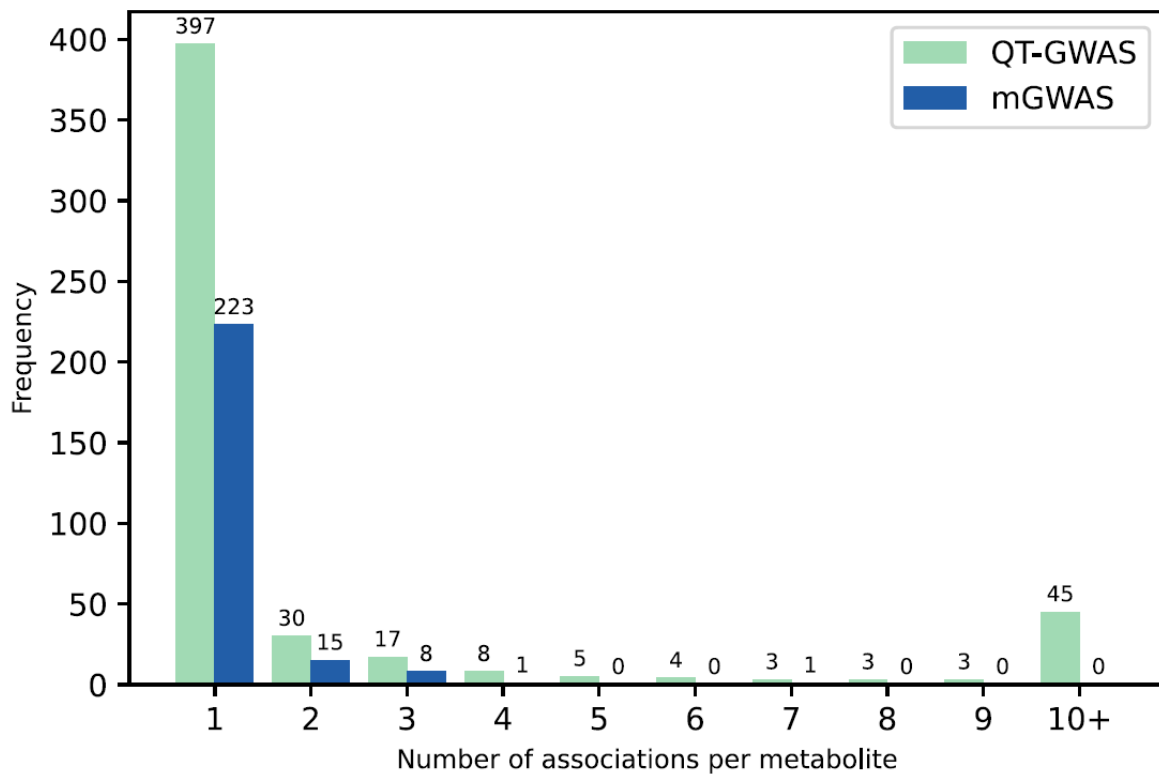


Figure 2: Distribution plot of the number of associations per metabolite retrieved for the 515 metabolites in the QT-GWAS (blue) and the 248 in the mGWAS (green). Of the 515 metabolites associated in QT-GWAS, 397 show an association with one locus, 118 with two or more loci. In mGWAS, 223 metabolites showed an association with one locus and 25 to multiple loci.

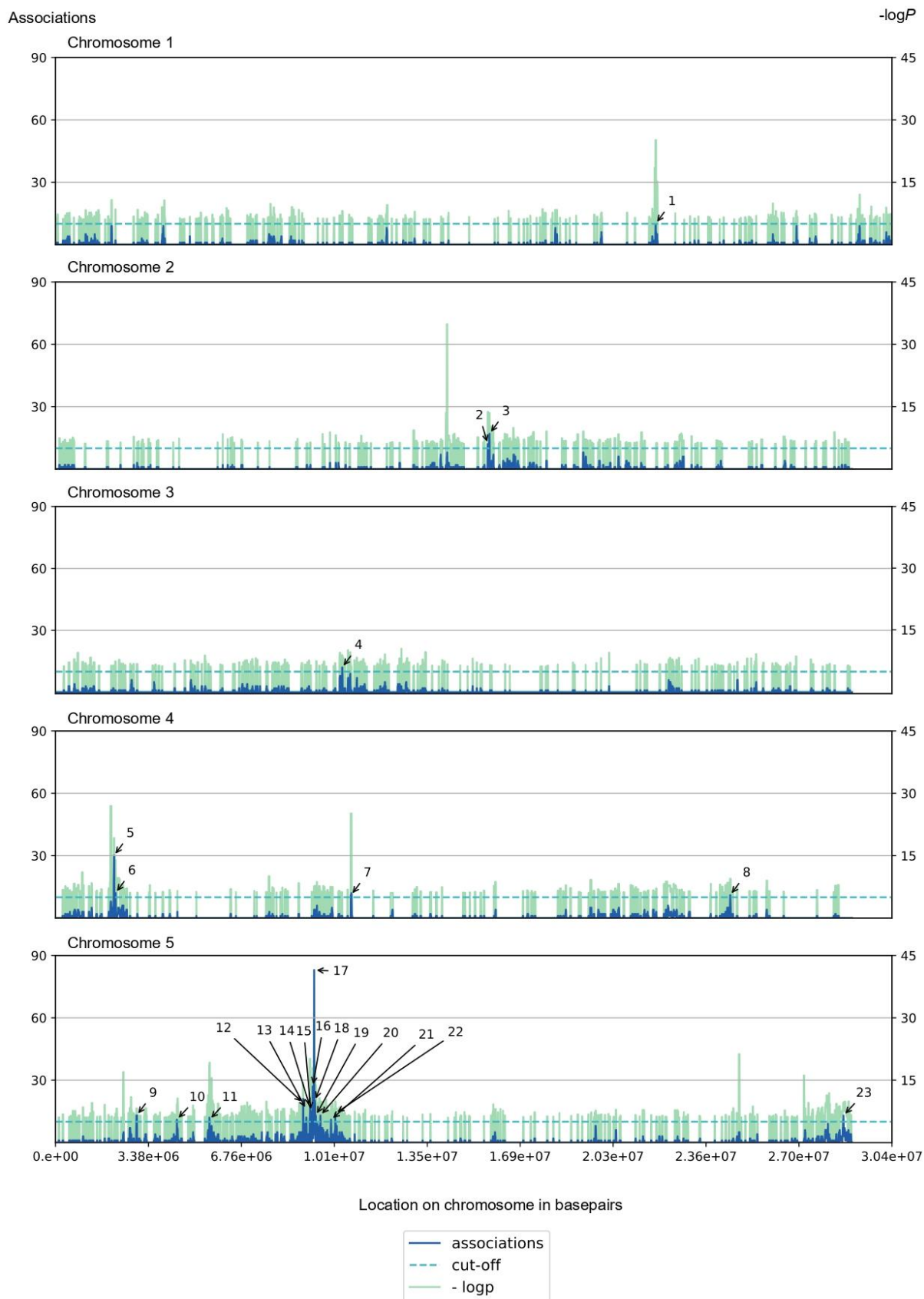


Figure 3: Overview of the pleiotropic loci (> 10 associations) obtained with the QT-GWAS. For each locus, the number of associations is represented in dark blue,

the negative logarithmic P -value with base 10 ($-\log P$) of the association in green. The dashed line represents the cut-off of ten associations to qualify as a pleiotropic locus. Pleiotropic loci are numbered according to Supplemental Table S3. A locus is defined as the region 10-kb upstream and 10-kb downstream of the most significant SNP (lead SNP) associated with a particular metabolite.

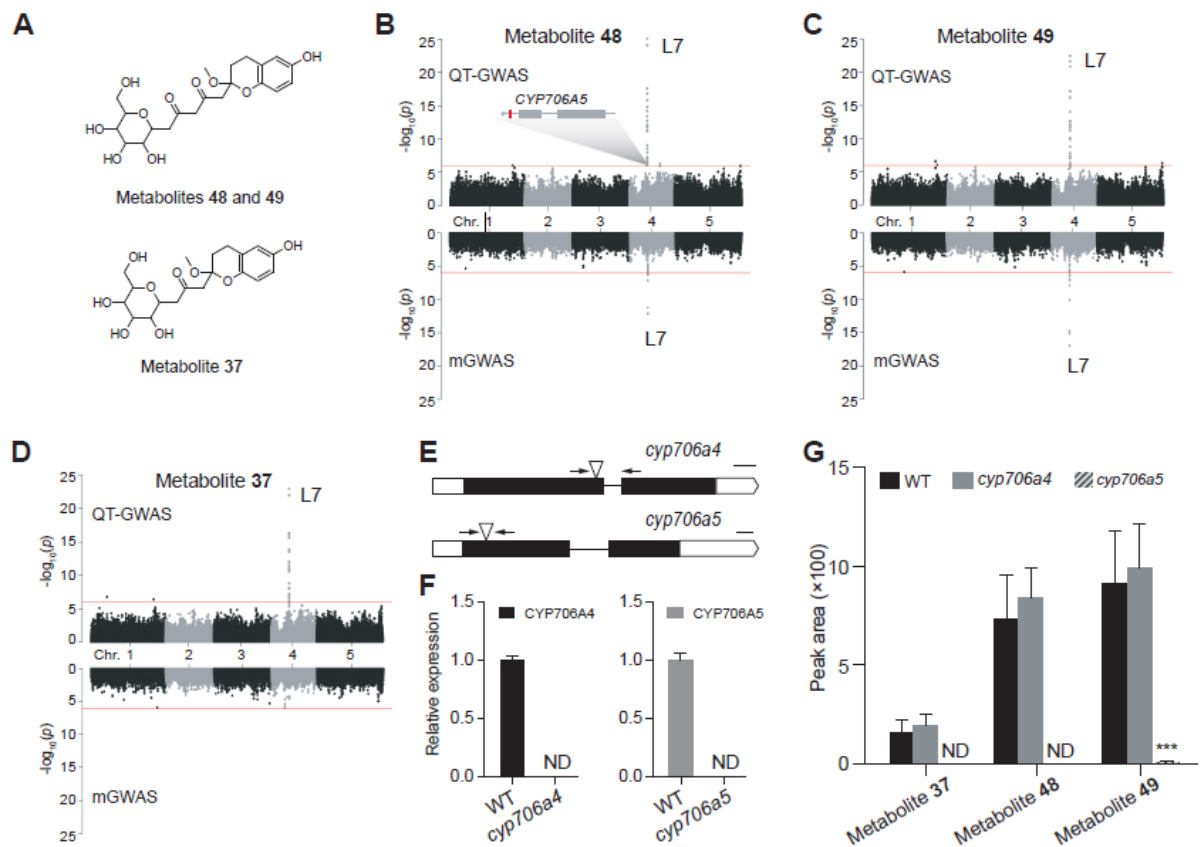


Figure 4: Overview of the *CYP706A* locus and its associated metabolites. A: putative structure of associated metabolites **48**, **49** and **37**. **B**, **C**, **D**: Manhattan plots of metabolites **48**, **49** and **37** respectively, for QT-GWAS (upper panel) and mGWAS (lower panel): the x-axis represents the location of the recorded SNPs on the genome, the y-axis represents the negative logarithmic P -value for the association of each SNP to the respective metabolites. **E**. Schematic representation of *CYP706A4* and *CYP706A5*; intronic regions are represented by a line, exonic regions are indicated in black and UTR regions in white; T-DNA insertion locations of the mutant lines are indicated by the triangles; Scale bar indicates 100 basepair. **F**. Relative expression of *CYP706A4* and *CYP706A5* as determined by RT-qPCR, primers are indicated by the arrows. **G**. Comparative metabolite profiling shows a significant reduction in the abundance of metabolites **37**, **48** and **49** in *cyp706a5* uniquely. Data are presented as mean \pm standard deviation, $n = 5$; ND, not detected. *** P -value < 0.001

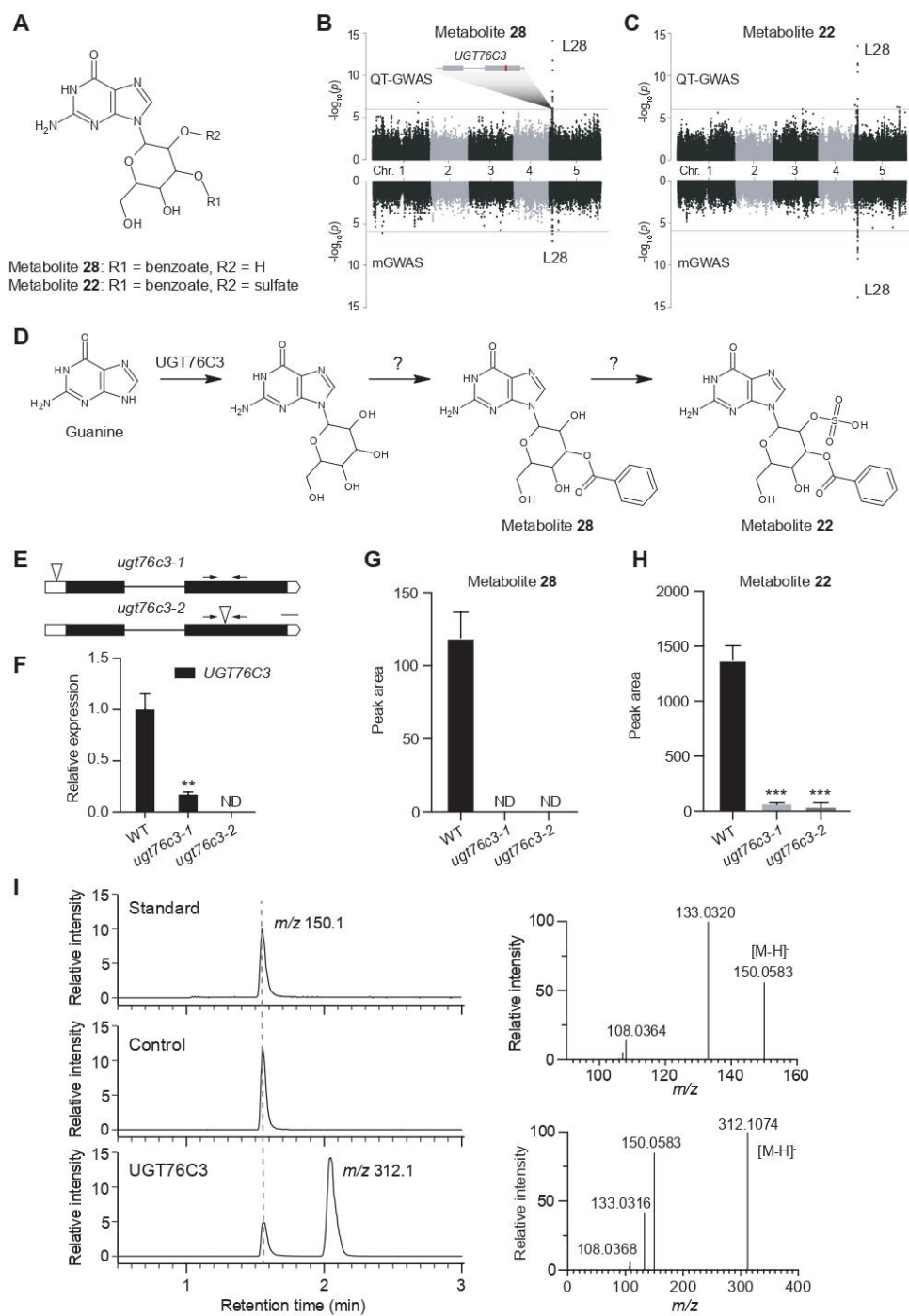


Figure 5: Overview of the *UGT76C* locus and its associated metabolites. A: putative structure of associated metabolites **28** and **22**. The sugar moiety is *N*-linked,

but its exact position and that of the substituents R1 and R2 are unknown. **B and C:** Manhattan plots of metabolites **28** and **22** respectively, for QT-GWAS (upper panel) and mGWAS (lower panel): the x-axis represents the location of the recorded SNPs on the genome, the y-axis represents the negative logarithmic *P*-value for the association of each SNP to the respective metabolites. A schematic representation of the candidate gene (*UGT76C3*) in L28 is shown and the most significantly associated SNP is marked in red within the gene. **D.** Proposed pathway for the biosynthesis of metabolites **28** and **22** in which *UGT76C3* catalyzes the first step, namely the hexosylation of guanine. **E.** Schematic representation of *UGT76C3*; intronic regions are represented by a line, exonic regions are indicated in black and UTR regions in white; insertion locations of the mutant lines are indicated by the triangles. **F.** Relative expression of *UGT76C3* as determined by RT-qPCR, primers are indicated by the arrows. **G and H.** Comparative metabolite profiling shows a significant reduction of metabolites **28** and **22** in both mutant lines. Data are presented as mean \pm SD, *n* = 5; ND, not detected. ****P*-value < 0.001, **0.001 < *P*-value < 0.01. **I.** *In vitro* enzyme assays show the conversion of guanine to guanine glucoside in the *UGT76C3* reaction exclusively (left panel). GST-tagged RFP was used as negative control. MS/MS spectral data confirmed the characterization of *m/z* 150.1 as guanine (right upper panel) and *m/z* 312.1 as guanine glucoside (right lower panel).

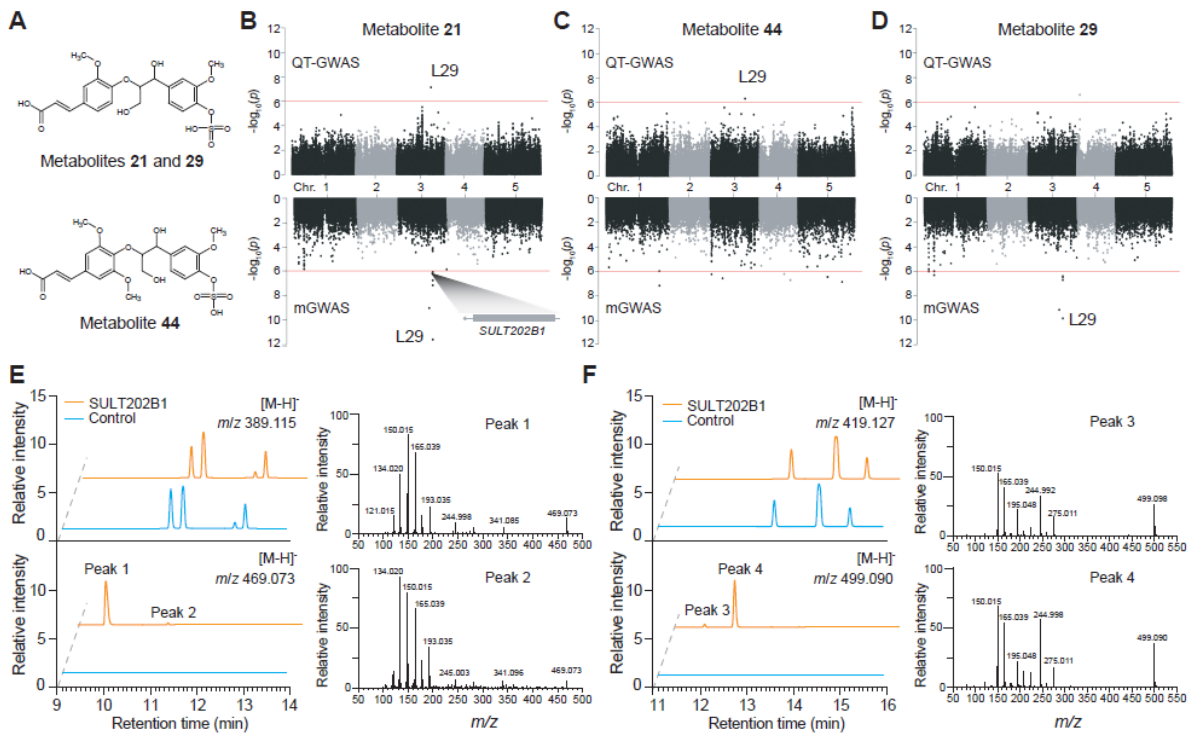


Figure 6: Overview of the *SULT202B1* locus and its associated metabolites. A. Putative structure of associated metabolites **21**, **29** and **44**. The exact position of the sulfate group could not be determined based on MS/MS spectral data. **B**, **C** and **D**: Manhattan plots of metabolites **21**, **44** and **29** respectively, for QT-GWAS (upper panel) and mGWAS (lower panel): the x-axis represents the location of the recorded SNPs on the genome, the y-axis represents the negative logarithmic *P*-value for the association of each SNP to the respective metabolites. The candidate gene (*SULT202B1*) in L29 is shown. **E** and **F**: Chromatograms of *in vitro* enzymatic reactions of *SULT202B1* with chemically synthesized G(8-*O*-4)FA and G(8-*O*-4)SA, respectively. GST-tagged RFP was used as negative control. MS/MS spectral data confirmed the characterization of two *m/z* 469.073 products (peaks 1 and 2) as sulfo-G(8-*O*-4)FA and two *m/z* 499.090 products (peaks 3 and 4) as sulfo-G(8-*O*-4)SA.

TABLES

Table 1: Overview of associations supported by literature and newly confirmed associations for QT-GWAS, mGWAS, and ASRgwas (population structure correction for qualitative metabolites). “No.” refers to the corresponding metabolite number as used in the text and Supplemental Table S2. “NA” indicates that no association was recorded for the corresponding method. FA, ferulic acid; SA, sinapic acid, ISF, detected as in-source fragment.

Gene	Metabolite name	No.	P-value		
			QT-GWAS	mGWAS	ASRgwas
Associations confirmed by previous research					
<i>DAAR1</i>	acetyl-(iso)leucine	18	1.10×10^{-27}	1.86×10^{-26}	7.41×10^{-11}
<i>MAM1/2/3</i>	3-methylsulfinylpropyl glucosinolate	1	1.58×10^{-8}	NA	0.019
	3-oxathiolesulfinylpropyl glucosinolate	2	NA	3.03×10^{-7}	NA
	butyl glucosinolate	6	4.03×10^{-8}	2.17×10^{-9}	0.022
	3-methylsulfinylbutyl glucosinolate	7	1.48×10^{-12}	NA	1.85×10^{-6}
	methylbutenyl glucosinolate	8	NA	2.86×10^{-7}	NA
	glutathionylated methylsulfinylhexyl glucosinolate	15	3.47×10^{-13}	NA	1.54×10^{-5}
	sulfohydroxyimidazolone-G(8-O-4)FA	17	3.56×10^{-11}	NA	2.17×10^{-3}
	dihydroxynonenyl glucosinolate	20	NA	9.64×10^{-7}	NA
	phenylpropyl glucosinolate	23	2.24×10^{-17}	NA	6.06×10^{-5}
	4-benzoyloxybutyl glucosinolate	40	1.92×10^{-10}	8.67×10^{-18}	8.55×10^{-9}
7-methylthioheptyl glucosinolate	47	1.38×10^{-8}	2.69×10^{-7}	4.80×10^{-4}	
<i>AOP3</i>	3-oxathiolesulfinylpropyl glucosinolate	2	8.14×10^{-12}	8.92×10^{-7}	5.95×10^{-5}
	4-O-sulfo-G(8-O-4)FA (isomer)	29	2.48×10^{-7}	NA	9.24×10^{-6}
<i>GSL-OH/2OG</i>	glutathionylated methylsulfinylhexyl glucosinolate	15	3.14×10^{-8}	NA	9.00×10^{-5}
	sinapoyl-(4-O-hexosylsinapoyl)-hexose	34	9.30×10^{-9}	NA	8.78×10^{-4}
	sinapoyl hexose(8-8)S ^{red}	42	4.13×10^{-9}	NA	5.01×10^{-5}
<i>BGLU6</i>	quercetin-3-O-hexosyl(1->6)hexoside-7-O-deoxyhexoside	19	5.72×10^{-23}	5.80×10^{-10}	3.60×10^{-4}
	kaempferol-3-O-hexosyl(1->6)hexoside-7-O-deoxyhexoside	25	1.49×10^{-24}	9.13×10^{-9}	2.09×10^{-11}
	isorhamnetin-3-O-hexosyl(1->6)hexoside-7-O-deoxyhexoside	27	3.50×10^{-25}	NA	3.32×10^{-11}
Associations supported by previous research					
<i>GH3</i>	12-hydroxy-4,5-didehydrojasmonoyl glutamine hexoside	24	1.50×10^{-15}	4.62×10^{-19}	2.71×10^{-11}
	12-hydroxy-4,5-didehydrojasmonoyl glutamine hexoside (isomer)	26	2.34×10^{-19}	2.19×10^{-14}	4.18×10^{-5}
	12-hydroxy-4,5-didehydrojasmonoyl glutamine hexoside (isomer)	30	1.25×10^{-15}	1.94×10^{-17}	2.79×10^{-8}
	12-hydroxy-4,5-didehydrojasmonoyl glutamine	45	6.04×10^{-20}	4.68×10^{-9}	4.54×10^{-5}
	malonyl (2-hydroxy-4,5-didehydrojasmonoyl glutamine)	46	1.06×10^{-12}	1.65×10^{-10}	8.19×10^{-5}
<i>SCPL13/8/9</i>	sinapoyl-(4-O-hexosylsinapoyl)-hexose	34	3.96×10^{-9}	NA	7.00×10^{-4}
Newly confirmed associations					

<i>CYP706A5</i>	6-hydroxy-2-methoxy-2-(2'-propanone-C-hexoside)-chroman	37	1.12×10^{-23}	NA	2.88×10^{-11}
	6-hydroxy-2-methoxy-2-(pentane-2',4'-dione-5'-C-hexoside)-chroman	48	7.12×10^{-26}	7.41×10^{-13}	5.11×10^{-12}
	6-hydroxy-2-methoxy-2-(pentane-2',4'-dione-5'-C-hexoside)-chroman (isomer)	49	3.44×10^{-23}	1.03×10^{-17}	1.02×10^{-12}
<i>UGT76C3</i>	guanine (benzoyl) sulfohexoside	22	3.25×10^{-14}	1.37×10^{-14}	5.11×10^{-4}
	guanine (benzoyl) hexoside	28	1.17×10^{-17}	1.02×10^{-7}	2.25×10^{-9}
<i>SULT202B1</i>	sulfo-G(8-O-4)FA	21	7.37×10^{-8}	2.55×10^{-12}	6.07×10^{-7}
	sulfo-G(8-O-4)FA (isomer)	29	NA	1.40×10^{-10}	NA
	sulfo-G(8-O-4)SA	44	4.92×10^{-7}	NA	3.43×10^{-5}